THE UNIVERSITY OF CHICAGO

CEREBELLAR PHYSIOLOGICAL ABNORMALITIES IN THE 15Q11-13 DUPLICATION AND CYFIP1 OVEREXPRESSING MURINE MODELS OF AUTISM SPECTRUM DISORDER

A DISSERTATION SUBMITTED TO

THE FACULTY OF THE DIVISION OF THE BIOLOGICAL SCIENCES

AND THE PRITZKER SCHOOL OF MEDICINE

IN CANDIDACY FOR THE DEGREE OF

DOCTOR OF PHILOSOPHY

COMMITTEE ON NEUROBIOLOGY

BY

DANA HEATHER SIMMONS

CHICAGO, ILLINOIS

DECEMBER 2018

Table of Contents

List of Figures

List of Abbreviations

4EGI-1	α-[2-[4-(3,4-Dichlorophenyl)-2-thiazolyl]hydrazinylidene]-2-nitro-benzenepropanoic acid
ACSF	Artificial Cerebrospinal Fluid
AMPA	α-amino-3-hydroxy-5-methyl-4-isoxazolepropionic acid
ANOVA	Analysis of Variance
Arc	Activity-Regulated Cytoskeleton-Associated Protein
ASD	Autism Spectrum Disorders
ATP	Adenosine Triphosphate
$CaCl_2$	Calcium Chloride
Cbln1	Cerebellin-1 (murine protein)
CF	Climbing Fiber
CO_2	Carbon Dioxide Gas
CsCl	Cesium Chloride
CYFIP1	Cytoplasmic FMR1-Interacting Protein 1
CYFIP1	Human gene coding for the CYFIP1 protein
CX546	CX546
EDTA	Ethylenediaminetetraacetic Acid
EGTA	ethylene glycol-bis(β-aminoethyl ether)-N,N,N',N'-tetraacetic acid
eIF4E	Eukaryotic Translation Initiation Factor 4e
eIF4G	Eukaryotic Translation Initiation Factor 4g
Eif4ebp2	Murine gene coding for the eIF4e protein
EPSC	Excitatory Postsynaptic Current
EPSP	Excitatory Postsynaptic Potential
FMRP	Fragile X Mental Retardation Protein
G	Calcium-Sensitive Fluorescence
GABA	γ-aminobutyric acid
Gluδ2	Glutamate δ2
GTP	Guanosine Triphosphate
HEPES	4-(2-hydroxyethyl)-1-piperazineethanesulfonic acid
HRP	Horseradish Peroxidase
KCl	Potassium Chloride
KO	Knock-out
KOH	Potassium Hydroxide
LTP	Long-Term Potentiation
LTD	Long-Term Depression
matDp/+	Maternally Duplicated
$MgCl_2$	Magnesium Chloride
mGluR1	Metabotropic Glutamate Receptor 1
mTOR	Mechanistic Target of Rapamycin
$NaHCO_3$	Sodium Bicarbonate
Na_2HPO_4	Disodium Phosphate
NaCl	Sodium Chloride
NMDA	N-methyl-D-aspartate
O_2	Oxygen Gas

OE	Overexpressing
P	Postnatal day
patDp/+	Paternally Duplicated
PBS	Phosphate Buffered Saline
PF	Parallel Fiber
PFA	Paraformaldehyde
PFb	Parallel Fiber Burst
PF-LTP	Long-Term Potentiation at the PF-Purkinje Cell Synapse
PF-LTD	Long-Term Depression at the PF-Purkinje Cell Synapse
PKCγ	Protein Kinase Cγ
PPF	Paired-Pulse Facilitation
PPR	Paired-Pulse Ratio
R	Baseline Fluorescence
RT	Room Temperature
RT-PCR	Real Time Polymerase Chain Reaction
SEM	Standard Error of the Mean
TSC	Tuberous Sclerosis Protein
TRIS	Tris(hydroxymethyl)aminomethane
TX	Triton
Ube3a	Ubiquitin-Protein Ligase E3A (murine protein)
UBE3A	Ubiquitin-Protein Ligase E3A (human protein)
USVs	Ultrasonic Vocalizations
VGluT1	Vesicular Glutamate Transporter 1
VGluT2	Vesicular Glutamate Transporter 2
WT	Wild-Type

Acknowledgements

I would like to thank Christian Hansel for his mentorship and support in encouraging me to think critically about how to interpret data, design meaningful scientific projects, and grow as a scientist. Thank you to the past and present members of the Hansel lab including Heather Titley, Giorgio Grasselli, Gabrielle Watkins, and Daniel Gill for their advice, friendship, thoughtful discussions, and musings about LTD. I would like to thank the members of my thesis committee, Peggy Mason, Sam Sisodia, and Wei Wei, for their mentorship and guidance, for asking the tough questions in order to help me think through my experiments, and for fostering my development as a scientist.

Thank you to Ben Marcus for being my loving, supportive husband, whether it means celebrating my excitement about a successful experiment, or helping me navigate a challenge. Ben, you help me grow personally, and always push me to achieve my goals. I'm so glad you invited me to dinner on my very first day in Hyde Park!

I would like to thank Marissa Simmons for her moral support and sisterly love, and for always lending an ear to hear about my experiments and getting excited about my science-art.

To Maddie Beagle Simmons and S'mores Shivakumar Simmons Marcus, thank you for your love and warmth, for brightening each of my days, and for always being there for me.

To my parents, Jody and Rick Simmons, thank you for loving and supporting me from the very beginning. I would not be where I am today without your guidance in helping me develop my work ethic, integrity, and drive to always do my best. Thank you for cultivating my individuality as a pink and sparkly scientist. Thank you for listening to me chat about Purkinje cells for six years, for learning all about ballet, for celebrating my life goals and choices, and for always reminding me to be kind and keep it real.

Technical Abstract

Autism Spectrum Disorders (ASD) present a range of symptoms including abnormal social interactions, increased perseverative behaviors, and difficulty with communication. Despite the many studies on these classical symptoms, many patients also display underestimated motor symptoms. Motor symptoms such as impaired motor learning during eyeblink conditioning, as well as difficulty with eye movements and unstable gait or coordination, are strong evidence for cerebellar involvement in the pathology of ASD. Eyeblink conditioning is dependent on an intact, functional cerebellar circuit. Disrupted eyeblink conditioning in the ASD patient population suggests that ASD is a synaptic disorder, and that the cerebellar circuit is impaired and must be interrogated to understand ASD motor symptoms at a synaptic level (Piochon et al 2014).

To examine synaptic changes in ASD, I used the mouse model of the human 15q11-13 copy number variation duplication. The human 15q11-13 chromosomal region is syntenic to part of mouse chromosome 7. In these mice, mouse chromosome 7 is duplicated to simulate the autistic-like phenotype. The 15q11-13 model represents the most frequent and penetrant genetic aberration in ASD and is seen in approximately 1-3% of patients. Patients inheriting this duplication maternally show symptoms of ASD, while patients receiving the genetic aberration paternally either do not show symptoms, or show them to a lesser degree. In the mouse model, the opposite is true; mice inheriting the duplication paternally (patDp/+), but not maternally (matDp/+), show autistic-like symptoms.

It is known that long-term depression at parallel fiber (PF) – Purkinje cell synapses (PF-LTD), which is a synaptic plasticity mechanism underlying eyeblink conditioning, is impaired in patDp/+ mice (Piochon et al 2014). To determine which part of the PF-LTD induction protocol

failed, I measured PF-evoked excitatory postsynaptic potentials (EPSPs) and climbing fiber (CF) – evoked excitatory postsynaptic currents (EPSCs) with patch clamp electrophysiology. I found that in patDp/+ mice, PF-EPSP amplitudes were decreased, while CF-EPSC amplitudes were enhanced, relative to wild-type (WT) littermates.

Immunohistochemistry for the vesicular glutamate transporter at CF-Purkinje cell synapses (VGluT2), confirmed that CFs make more synapses onto Purkinje cells in patDp/+ mice than in WT littermates. Importantly, these CF-Purkinje cell synapses, which are typically found on large caliber dendrites, were ectopically located on fine dendrites in patDp/+ mice. Fine dendrites are generally considered territory for PF-Purkinje cell synapses (Palay & Chan-Palay 1974, Ichikawa et al 2002, Watanabe et al 2008, Miyazaki et al 2010). To explore whether this territorial change affected calcium signaling through PF-Purkinje cell and CF-Purkinje cell synapses, I performed spine calcium imaging at PF spines and measured transients resulting from three stimulation protocols: 100 Hz PFb, CF, and 100 Hz PFb+CF (PF-LTD induction protocol). Notably, I found that PF-evoked calcium transients were significantly reduced in amplitude in patDp/+ mice. Weak calcium signaling at PF-Purkinje cell synapses suggests that PF signaling is too weak to induce PF-LTD in patDp/+ mice.

To test whether PF-evoked calcium signaling was insufficient to induce PF-LTD, we performed LTD experiments in WT mice, patDp/+ mice – which leads to potentiation instead of depression, and patDp/+ mice with ACSF containing 300 μm CX546. CX546 modulates α-amino-3-hydroxy-5-methyl-4-isoxazolepropionic acid (AMPA) receptors to promote prolonged depolarization, which causes voltage-gated calcium channels to open. Effectively, CX546 increases postsynaptic calcium influx. The addition of CX546 sufficiently increased calcium

entry to Purkinje cells in patDp/+ mice during the PF-LTD induction protocol and successfully restored PF-LTD in patDp/+ mice.

Finally, the 15q11-13 chromosomal region contains approximately 20 genes. I sought to identify the involvement of these genes in ASD symptoms. I explored ubiquitin-ligase E3A, (Ube3a), a gene that when deleted is responsible for Prader-Willi and Angelman Syndromes (Albrecht et al 1997) and found that Ube3a is upregulated in patDp/+ mice relative to WT littermates. Additionally, I explored cytoplasmic FMR1-Interacting Protein 1 (CYFIP1) using mice that globally overexpress (OE) CYFIP1 because the protein is upregulated in ASD patients. CYFIP1 OE mice displayed a slight enhancement in the amplitude of CF-EPSCs. Continued experiments on both mouse models will lead to better understanding of ASD as a synaptic disorder that involves motor pathology. Examination of motor pathology may lead to earlier diagnosis of ASD and earlier behavioral therapeutic interventions.

Chapter 1: General Introduction

Introduction to Autism Spectrum Disorders

ASD is typically characterized by deficits in social interactions, increases in repetitive or compulsive behaviors, and difficulties with communication. ASD affects individuals over a wide range of IQ levels with symptoms that can be debilitating and severe, barely noticeable, or anywhere in the middle. Since ASD encompasses a wide range of symptoms, there is extensive variation among the patient population. It has been observed that ASD affects approximately 1% of people in the United States, and that about four times as many males as females show classical behavioral symptoms of ASD (Zoghbi & Bear 2012).

Beyond the classical ASD symptoms though, one often overlooked, but highly reliable symptom of ASD is rarely explored: motor pathology. Approximately 80% of patients with ASD show motor pathology (Green et al 2009, Fournier et al 2010) that includes clumsy gait, unsteady balance, and difficulty with eye contact and eye movements (Johnson et al 2013, Mosconi et al 2013) – all of which provide strong evidence for cerebellar dysfunction in ASD. Motor symptoms involving eye movements and eye contact often appear at an earlier age than the typical diagnosis age for ASD, which is between 1.5-3 years. The early presentation of motor pathology may make these symptoms useful as a reliable biomarker for earlier diagnosis of ASD (Reeb-Sutherland, Fox 2015). Early diagnosis would facilitate a pathway for early behavioral intervention, thus improving the lives of ASD families.

One particular motor deficit that has been studied experimentally in human patients is eyeblink conditioning. Patients were unable to learn to associate a conditioned stimulus (tone or light) with a co-terminating unconditioned stimulus (air puff) as well as their typically behaving, healthy counterparts could (Sears et al 1994, Oristaglio et al 2013). Although blinking during an

experiment is not the most socially-relevant or important symptom in the lives of ASD patients, it is nonetheless useful in an experimental context because the cerebellar circuitry underlying eyeblink conditioning is well understood (McCormick and Thompson 1984). Deficits in eyeblink conditioning indicate strong evidence for reliable involvement of the cerebellum in ASD pathology (McCormick and Thompson 1984). Indeed, several recent studies have shown that the cerebellum is one of the most consistently affected brain regions in ASD (Fatemi et al 2012). Anatomically, ASD has been linked to abnormal cerebellar morphology including floccular dysplasia (Wegiel et al 2013), hypoplasia of the vermis (Courchesne 1997, Carper & Courchesne 2000, Kaufmann et al 2003), and Purkinje cell degeneration (Palmen et al 2004).

Advantages of the Cerebellum for ASD Research

The cerebellum is a critical brain region to study in ASD research for several reasons: the circuitry is well understood, the relationship between synaptic plasticity and eyeblink conditioning has been studied extensively (McCormick & Thompson 1984), and the structure has been conserved relatively well compared with other brain regions over vertebrate evolution (Bell 2002).

The cerebellum is a highly organized structure in the hindbrain that receives inputs from the motor cortex, the premotor cortex, primary and secondary sensory cortices, secondary visual areas in the posterior parietal lobe, and the inferior olive (Purves et al 2001). These cortical inputs all arrive at the cerebellum indirectly via the pontine nuclei. Additional inputs that are indirect and arrive at the cerebellum through the pre-cerebellar nuclei include somatosensory and spinal inputs. The cerebellum also receives direct sensory inputs from the vestibular system and the medulla oblongata. After processing input signals, the cerebellar cortex projects information

out through Purkinje cell axons to the deep cerebellar nuclei (includes dentate, interposed, and fastigial nuclei) and vestibular nuclei, which in turn project to motor neurons, the thalamus, and the spinal cord (Purves et al 2001).

The principle cell type in the cerebellar cortex is the Purkinje cell, a neuron that displays an impressively intricate dendritic arbor. Importantly, the Purkinje cell is the only cell that projects out of the cerebellar cortex. During the first month of development, the dendritic arbor grows and flattens into a monoplanar shape with sagittal orientation (Kaneko et al 2011). Purkinje cells receive input from two glutamatergic sources: CFs and PFs. CFs originate as inferior olivary neurons in the medulla oblongata whose axons reach through the inner granular layer of the contralateral cerebellar cortex (Sugihara et al 1999). The axon of the inferior olivary neuron branches into multiple CFs, and each one of these CFs innervates one single Purkinje cell (Armstrong & Schild 1970). One CF makes hundreds to thousands of synapses onto a single Purkinje cell (Rossi et al 1993), and produces a large postsynaptic depolarization event upon excitation (Eccles et al 1966). In the molecular layer, the CF innervates primary, large caliber dendrites of the Purkinje cell, but does not typically innervate higher order, fine dendrites (Sugihara et al 1999).

PFs provide the other source of glutamatergic input to Purkinje cell dendrites. PFs are the axons of granule cells, whose somata reside in the granular layer of the cerebellar cortex. Granule cells are innervated by mossy fibers, which carry signals from the cerebral cortex, the vestibular nuclei, the reticular formation, and the spinal cord. Granule cell axons extend up from the granular layer into the molecular layer, and then project PFs orthogonally through the nearly-flat Purkinje cell dendrites. The signal carried in one PF is received by several hundred Purkinje cells along the length of the folia (Goodlett & Mittleman 2017). Typically, PFs innervate the

higher order, or fine, dendrites of Purkinje cells in the outer portion of the molecular layer (Ichikawa et al 2002).

Extensive knowledge of the cerebellar circuit has enabled researchers to uncover remarkable links between proteins, synaptic transmission, synaptic plasticity, and behavior. The ability to study a behavior over so many different levels of complexity is a major advantage of using the cerebellum in research. The rigid organizational structure of the cerebellar cortex has allowed researchers to study, perturb, and interrogate the circuit extensively, and has led to insights about the mechanisms underlying cerebellum-dependent behaviors such as eyeblink conditioning. Eyeblink conditioning, and the ability of a vertebrate test subject (mouse and human are discussed here) to learn to associate a conditioned stimulus with a co-terminating unconditioned stimulus on a millisecond timescale, depends on intact cerebellar function (McCormick and Thompson 1984). In the delay eyeblink conditioning test, when the subject correctly learns the association, he or she will blink in order to avoid a startling and unexpected air puff (unconditioned stimulus) from reaching the eye. A mouse or patient who fails to associate the stimuli with the correct timing will not blink, or will blink at the incorrect time (Review: Freeman and Steinmetz 2011). In addition to patients showing difficulties with learning eyeblink conditioning, Kloth and colleagues found that autistic-like mice from four distinct mouse models were less likely to form a correct conditioned response during the delay eyeblink conditioning test (15q11-13, Cntnap2-/-, L7-Tsc1, and Shank3+/ΔC, Kloth et al 2015).

Proper eyeblink conditioning requires plasticity in the cerebellar cortex, and has been associated with synaptic plasticity at the PF-Purkinje cell synapse (Piochon et al 2014). In the study, data confirmed the hypothesis from Jörntell and Hansel's 2006 report that PF-LTD, a main cerebellar synaptic plasticity learning mechanism, occurs when a subject learns the

association required to blink at the right time during this task, and that PF-LTP is associated with extinction training, during which a subject actively forgets or "unlearns" the association between the stimuli. PF-LTD and PF-LTP can be considered putative cellular correlates of conditioned response acquisition and extinction respectively (Marr 1969, Albus 1971, Ito 1984, Jörntell & Hansel 2006). In cerebellar synaptic plasticity, it is important to note that activation of the CF is required in order to provide the large calcium influx that is mandatory for inducing PF-LTD (Coesmans et al 2004). The CF is often considered an "error signal" which will change its firing pattern when motor learning, or a real-time motor adjustment is needed (Simpson et al 1996, De Zeeuw et al 1998, Najafi & Medina 2013). In contrast, PF-LTP only requires the activation of PFs, which provide less calcium influx to postsynaptic Purkinje cells (Coesmans et al 2004).

A second major advantage of studying the cerebellum is that it has been relatively conserved (compared with brain regions such as the neocortex) over the course of vertebrate evolution (Bell 2002). Importantly, the circuitry underlying eyeblink conditioning in the murine brain is the same as the circuitry underlying the same exact behavior in the human brain (Thompson & McCormick 1984). Since eyeblink conditioning is not an invasive experiment, it can and has been used on human test subjects, including ASD patients (Sears et al 2004, Oristaglio et al 2013). This unparalleled, albeit indirect, access to brain circuitry underlying a human behavior enables researchers to draw conclusions about the human cerebellum. Since the cerebella of humans and mice are relatively similar, more invasive studies that would be unethical to perform on humans are done using mice.

Murine Models of ASD

The use of mice in research studies continually provides access to valuable information that cannot be obtained without performing invasive studies. While it would be ideal to learn about brain circuitry and disorders by using a constructed model of the human brain, there is not enough known about the brain to make this ideal a reality. To date, one must examine an actual brain in order to learn about the brain. For obvious ethical reasons, live human brains cannot be extracted for research studies. The extraction of mouse brains for research studies has become the accepted practice by the research community in lieu of a legitimate alternative. The advantages of working with mice are numerous: they have a short breeding time, their genome can be easily manipulated, and they are relatively inexpensive compared to other animals because of their short generation cycles. Notably, the most important advantage is that murine cerebellum bears striking similarity to the human cerebellum.

Despite the benefits of using mice to understand brain function and dysfunction, it is essential to keep in mind the fact that a mouse is not a human. A mouse will never show behavior as complex as a human will, which brings up the question of, "How can a human disorder be studied in a mouse?" While a mouse indeed has a different behavioral paradigm than a human, it has been suggested that the mouse behavioral repertoire has homologs for some human behaviors (Simmons et al, *in preparation*). For example, a patient with ASD may show symptoms including repetitive or compulsive behaviors such as flipping light switches or washing his or her hands repeatedly. A mouse is unlikely to ever flip a light switch, but will display other repetitive behaviors that can be quantified such as self-grooming (Review: Kalueff et al 2016), digging, or burying marbles (Deacon 2006, Angoa-Pérez et al 2013). Similarly, a patient with ASD may show difficulty with communication. One way mice communicate with

each other is through the use of ultrasonic vocalizations (USVs). Often, USVs are emitted by pups when they are separated from their mother as an indication of stress (Noirot 1966, Scattoni et al 2009). A somewhat analogous human behavior is a human baby crying when stressed or separated from his or her mother. Abnormalities in USV frequency (both USVs/minute and pitch), duration, and intensity can be recorded and quantified. A third core symptom of ASD that many patients display is impaired social interactions, or a lack of interest in socialization. The social interests of mice have classically been quantified using variations of the three-chamber test (Dere et al 2007, Review: Silverman et al 2010, Kaidanovich-Beilin et al 2011). A typically behaving mouse will spend more time in the chamber with the social stimulus, but an autistic-like mouse will not (Review: Silverman et al 2010, Moy et al 2004).

All of these murine behaviors bear underlying similarity to the human behaviors, which makes them useful to study. However, these behaviors – even in mice – are complex, and the mechanisms behind them remain poorly understood. In contrast, the use of eyeblink conditioning is advantageous because the same exact test can be performed on the same behavior in both humans and mice, and the brain circuitry controlling the behavior is strikingly similar.

15q11-13 Mouse Model of ASD: In order to study the cerebellar circuitry underlying motor deficits in ASD, I used two different mouse models of ASD. The first mouse model of ASD bears a short interstitial duplication for the human 15q11-13 chromosomal region and was created in the laboratory of Dr. Toru Takumi at the RIKEN Brain Science Institute in Wako, Japan (Figure 1, Nakatani et al 2009). In the mouse model, a region of mouse chromosome 7 is duplicated as the copy number variation mutation because the region is syntenic to the human 15q11-13 chromosomal section. The model was selected because it recapitulates a copy number

variation duplication seen in 1-3% of ASD patients (Cook & Scherer 2008). This chromosomal aberration represents one of the most frequent and penetrant genetic abnormalities seen in ASD. The 15q11-13 model is subject to imprinting, meaning that paternal inheritance of the duplication leads to autistic-like symptoms in offspring (patDp/+), but maternal inheritance does not (matDp/+, Nakatani et al 2009). Curiously, the inheritance pattern is reversed in patients such that maternal, but not paternal, inheritance leads to ASD. Approximately 90% of patients with the maternal duplication show symptoms of ASD, while only approximately 50% of patients with the paternal duplication show symptoms of ASD (Cook & Scherer 2008, Urraca et al 2013). The causes for reversed imprinting between species are not well understood. Problematically, the percentage of patients exhibiting symptoms that have known maternal or paternal duplications is based on a study with a very small sample size: ten patients with a maternal duplication and only four patients with a paternal duplication (Urraca et al 2013). Although it would undoubtedly be useful for research studies to obtain genetic information from each ASD patient, it must be noted that doing extra testing in addition to behavioral therapy with very young ASD patients can be difficult. Most families elect not to subject their child with ASD to genetic testing. In contrast to working with patients, it is much more feasible to genotype mice and associate their mutation with affected physiology and behavior.

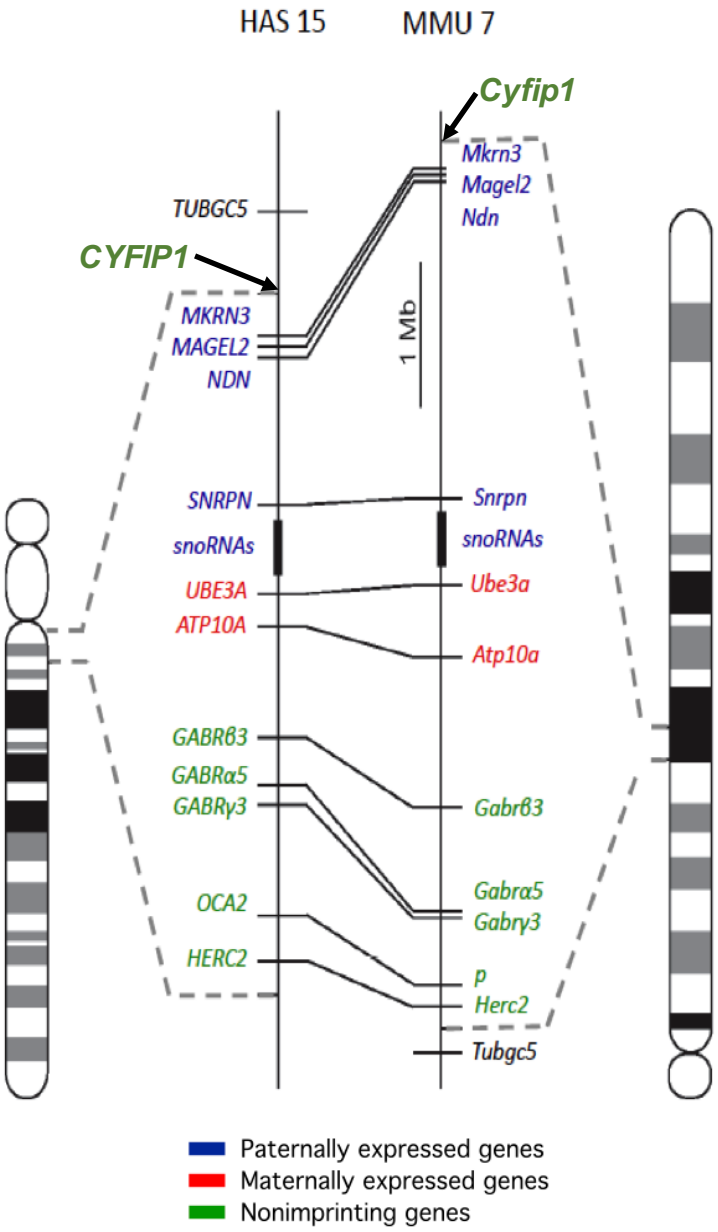

Figure 1: Conserved linkage group on human chromosome 15q11-13 and mouse chromosome 7. Schematic of conserved linkage group in the human and mouse chromosomes. The paternally expressed, maternally expressed, and non-imprinting genes are shown in blue, red, and green, respectively. Genomic segments that show linkage conservation in humans and mice are connected by dark shading if the gene orders are in the same direction relative to their respective centromeres. If the gene orders are in the opposite direction, they are connected by light shading. This figure is modified from Nakatani et al., *Cell* 137 (2009).

In addition to construct validity, patDp/+ mice from the 15q11-13 strain display strong face validity by showing difficulties with learning eyeblink conditioning and abnormalities in their gait parameters (Piochon et al 2014), as well as deficits in social interaction during the three-chamber test and abnormal USV communication (Nakatani et al 2009). Compiling a behavioral profile underscores the observation that patDp/+ mice display the mouse-equivalent of autistic-like core symptoms. Furthermore, patDp/+ mice provide strong construct validity since the genetic aberration is the most frequent genetic defect seen in ASD (Cook & Scherer 2008). In order to study the mechanisms behind abnormal eyeblink conditioning in these mice, Piochon and colleagues examined plasticity in the PF-Purkinje cell synapse and found that patDp/+ mice show deficient PF-LTD. Instead of decreasing the amplitude of EPSCs in response to tetanization, the amplitudes increased and showed potentiation (Piochon et al 2014). In this dissertation, I present my research into the components of the cerebellar circuit that are involved in the induction of PF-LTD in order to determine which part of the circuit underlies the deregulation of PF-LTD in patDp/+ mice.

The duplicated chromosomal region in the 15q11-13 mouse model of ASD encompasses approximately 20 genes. It is highly likely that combinations of these genes work together and affect ASD symptoms. In order to determine which of these genes might be involved in ASD pathology, I studied two genes within the duplicated region in isolation: UBE3A and CYFIP1.

UBE3A is a maternally expressed gene in humans, and is an attractive candidate gene for association with ASD pathology because its deletion leads to Angelman Syndrome (maternally deleted) and Prader-Willi Syndrome (paternally deleted, Albrecht et al 1997, Dindot et al 2008, Heck et al 2008). Deletions of UBE3A have also resulted in ASD-like symptomology in patients

with confirmed diagnoses of Angelman Syndrome or Prader-Willi Syndrome, suggesting comorbidity (Peters et al 2004).

It has been shown that increased UBE3A dosage in mice linearly enhances the severity of ASD-like symptoms such as impaired social behavior and abnormal glutamatergic synaptic transmission (Smith et al 2011). UBE3A is highly expressed in Purkinje cells at the synapse and nucleus (Dindot et al 2008), making it an important protein to examine in cerebellar studies involving potential synaptopathies. Within Purkinje cells, UBE3A acts as an E3A ligase that ubiquitinates other proteins, thereby targeting them to the lysosome for degradation. One such protein is Arc, an immediate early gene that is involved with synaptic plasticity (Guzowski et al 2000, Plath et al 2006, Okuno et al 2012, Wang et al 2016) and activity-dependent synaptic pruning during cerebellar development (Mikuni et al 2013).

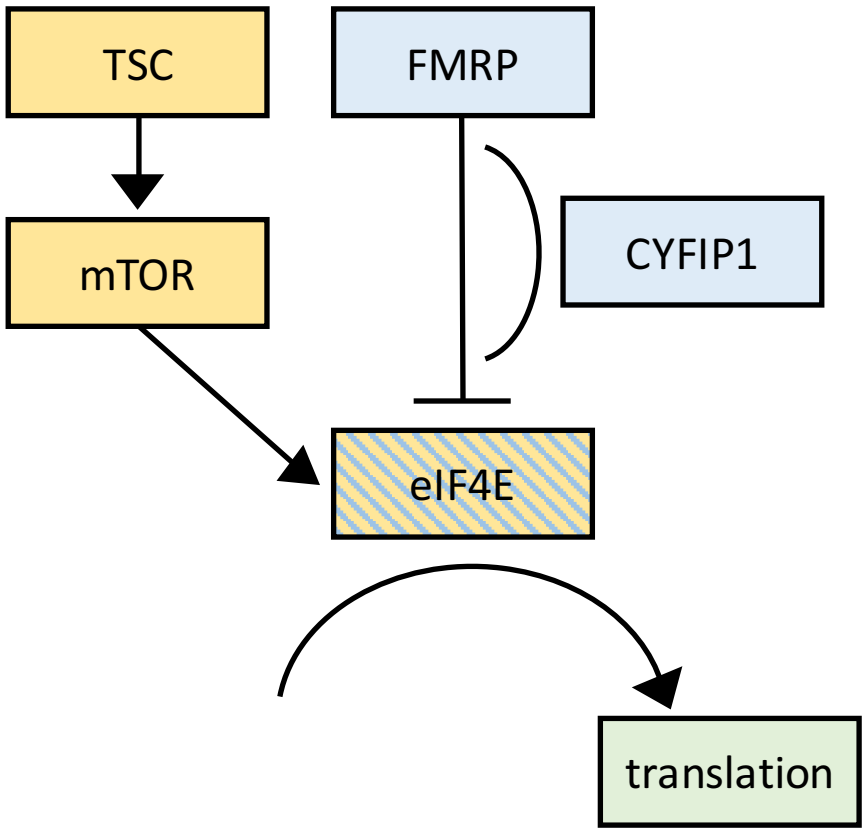

Figure 2: CYFIP1 prevents translation initiation in complex with FMRP and eIF4E.

Figure 2, continued. CYFIP1 prevents translation initiation in complex with FMRP and eIF4E. Increases in the tuberous sclerosis protein (TSC) enhance signaling in the mTOR pathway and promote translation by binding with eIF4E. In competition with this pathway, CYFIP1 binds FMRP and eIF4E, and together the protein complex represses translation at synapses. Yellow indicates promotion of translation, blue indicates repression of translation, green denotes the process of translation. Yellow and blue stripes indicate that eIF4E, when in complex with eIF4G, is part of pathways involving promoting and repressing translation.

CYFIP1 is a protein that represses the initiation of translation at the synapse through the mechanistic target of rapamycin (mTOR) pathway by binding to a complex that includes eukaryotic translation initiation factor 4E (eIF4E) and Fragile X Mental Retardation Protein (FMRP, Figure 2, Napoli et al 2008). Notably, overexpression of CYFIP1 protein was observed in post-mortem human brain tissue from ASD patients with the 15q11-13 duplication (Oguro-Ando et al 2015). To study a replication of this overexpression in mice, I used the CYFIP1 OE mouse model of ASD created by Dr. Daniel Geschwind's research group at the University of California at Los Angeles (Geschwind Lab, unpublished). The CYFIP1 OE mouse model of ASD is especially useful because it enables researchers to zero in on the overexpression of one specific gene within the 15q11-13 chromosomal region. The face validity of these CYFIP1 OE mice is currently being tested in the Geschwind Lab by determining whether the overexpressing mice show autistic-like symptoms including social deficits, increased repetitive behaviors, and abnormal communication. In this dissertation, I present the beginning of a physiological characterization of synaptic transmission in CYFIP1 OE mice at PF-Purkinje cell and CF-Purkinje cell synapses. The Geschwind lab previously showed overexpression of CYFIP1 leads to altered cell morphology including increased cell size, impaired neurite outgrowth, and enhanced spine density in pyramidal neurons (Oguro-Ando et al 2015). A different mouse model of ASD that bears a knockout for *Eif4ebp2*, a gene underlying translation initiation factor eIF4E that binds with the CYFIP1 protein, has been shown to display an increase in the ratio of

excitatory to inhibitory synaptic transmission. *Eif4ebp2* KO mice also showed ASD-like deficits in social behavior, abnormal time course of communication development, and increases in self-grooming repetitive behavior (Gkogkas et al 2013).

Chapter 2: Characterization of Abnormal CF- and PF-Purkinje Cell Connectivity and Function in 15q11-13 Mice

Introduction

ASD is a neurodevelopmental disorder in which symptoms begin to appear at around 18 months of age in patients. To understand what changes during development, and what leads to pathological symptoms, it is necessary to study the brain circuitry that underlies impaired behaviors during development. By testing behaviors with well-understood underlying circuitry, including eyeblink conditioning, we can decipher whether the circuitry is intact. The 15q11-13 patDp/+ mouse model of ASD represents one of the most frequent genetic abnormalities in ASD, and it exhibits impairments to eyeblink conditioning as well as deregulation of PF-LTD (Piochon et al 2014). The induction of PF-LTD requires co-activation of the PFs and the CF (Marr 1969, Albus 1971, Coesmans et al 2004, Piochon et al 2010, Schonewille et al 2010, Ito M et al 2014). CFs provide a large excitation of Purkinje cells, thereby opening N-methyl-D-aspartate (NMDA) receptors and voltage-gated calcium channels (Piochon et al 2007). This large calcium influx is necessary to induce LTD at the PF-Purkinje cell synapse (Coesmans et al 2004). In order to determine why PF-LTD is impaired in patDp/+ mice, I examined synaptic transmission of CFs and PFs in the cerebellar cortex.

At birth, each murine Purkinje cell is innervated by three or more CFs, which are competitively eliminated in an activity-dependent manner during development (Crépel et al 1976). By P21, most Purkinje cells in a WT mouse are innervated by one single CF each. The process of CF elimination has been studied extensively and is frequently used as a model of synaptic pruning during development (Reviews: Hashimoto and Kano 2013, Nishiyama 2015). The processes of selecting a "winning" CF, eliminating supernumerary CFs, and stabilizing the

synapses involves bidirectional activity-dependent signaling that includes C1qL1-Bai3 (anterograde, Kakegawa et al 2015), BDNF-TrkB (retrograde, Choo et al 2017), Progranulin to Sort1 (retrograde, Uesaka et al 2018), and Semaphorins 3A and 7A (retrograde, Uesaka et al 2014). The events modulating CF-elimination and translocation of the winning CF have been categorized into distinct temporal phases. Before P3, there are several equal-strength CFs on each Purkinje cell's soma. At this time, the molecular layer is still growing, and contains mostly PFs passing through the Purkinje cells' immature dendritic arbor (Ichikawa et al 2016). From P3-7, one CF is strengthened in an activity-dependent manner. This strengthened CF nearly always becomes the "winning" CF (Carillo et al 2013). From P7-9, the winning CF begins to translocate from the Purkinje cell soma onto the dendrites, making new, stable synapses along the way (Ichikawa et al 2016). P7-11 marks the early phase of CF-elimination, during which most of the extra CFs are retracted and removed. The early phase of elimination, as well as the selection of the winner, are mediated by P/Q-type voltage-gated calcium channels (Hashimoto et al 2011, Miyazaki et al 2004, Miyazaki et al 2012). P12-17 marks the late phase of CF-elimination, during which the winning CF continues to extend, and any remaining "losing" CFs are removed (Hashimoto & Kano 2013, Carillo et al 2013). By P21, each Purkinje cell will be innervated by one single CF and hundreds to thousands of PFs.

During adulthood, the CF typically innervates the large dendritic branches of Purkinje cells, and PFs typically innervate the higher order, fine dendritic branches (Palay & Chan-Palay 1974, Watanabe et al 2008). During P15-30, the area of overlap between the CF and the PFs on Purkinje cell dendrites is reduced, though never completely eliminated (Ichikawa et al 2002, Ichikawa et al 2016). How does this area of heterogeneous excitatory synaptic input to Purkinje cells develop? During development, and right before CF-elimination, granule cells grow and

their axons extend from the granular layer where their somata reside, into the molecular layer where they project their axons as PFs that are perpendicular to the Purkinje cell dendrites. In order for PFs to migrate into their territory and make synapses in the upper molecular layer, the PFs must compete with the CF to establish their segregated territories. Each neuron adds and removes synapses while migrating into position in a highly plastic manner. During the late phase of CF-elimination, metabotropic glutamate receptor 1 to protein kinase Cγ (mGluR1-PKCγ) signaling promotes the elimination of PF synapses from large caliber dendrites and the reduction in the size of the PF territory (Ichikawa et al 2016). As PF synapses are eliminated, the winning CF extends and fills in the space by making synapses onto the Purkinje cell dendrites (Ichikawa et al 2016). Still, the order of development remains unclear. Does the CF signal that it will begin to extend synapses into greater dendritic territory and cause PFs to retract their synapses and retreat, or *vice versa*? Does the CF extend into empty dendritic real estate after PFs have already retracted their synapses? Regardless, the end result is that the CF and PFs have mostly segregated territories with the CF synapsing onto large caliber dendrites, the PFs synapsing onto fine dendrites, and a small area of overlap in the middle (Watanabe et al 2008).

Though a great deal is known about the well-studied mechanism behind CF-elimination, few studies have explored the consequences of pathologically overgrown CFs on PF development, or rather the consequences of deficient PF signaling on CF elimination and growth. Is the overgrown CF invading PF territory such that PFs have no space left on the dendrites to make synapses? Or are the PFs weak and poorly connected, leaving empty space available on higher order dendrites for the CF to take over? In past studies, the *staggerer* mouse was shown to have persistent multiple innervation by CFs on Purkinje cells, and also showed a loss of granule cells (Crépel et al 1980). In other studies, intentional ablation or weakening of PFs has

led to a larger dendritic innervation area for CFs on Purkinje cells, as well as persistent multiple innervation (Kano et al 1998, Kurihara et al 1997, Hirai et al 2005, Watanabe et al 2008, Cesa & Strata 2009). My results show enhanced CF-Purkinje cell connectivity and excitation, as well as weak PF-Purkinje cell excitation in patDp/+ mice; however, it is still not clear which happens first.

Curiously, the process of CF-elimination in patDp/+ mice does indeed proceed to completion even though it has a delayed and extended time course relative to WT littermates (Piochon et al 2014). The lasting effects of this delayed pruning may include abnormal PF activity, impaired calcium signaling at the synapses, and a variety of downstream events.

Dysregulated synaptic transmission at CF- and PF-Purkinje cell synapses in patDp/+ mice indicates that it is useful to consider ASD as a synaptic disorder, or a synaptopathy (Peça et al 2011, review: Zoghbi & Bear 2012). Indeed, many genes implicated in ASD pathology have roles in synaptic structure and function (review: Zoghbi & Bear 2012). Importantly, an individual displaying synaptopathies during development may have deficiencies in synaptic plasticity. In turn, impaired synaptic plasticity in the cerebellum implies abnormal motor learning, which has already been observed in patDp/+ mice. Going forward, it will be important to examine other brain regions from mice showing autism-like symptoms in order to link faulty synaptic transmission with impaired plasticity, and link impaired plasticity with core symptoms of ASD such as abnormal communication, increased repetitive behaviors, and difficulty with social interactions. These core symptoms are relatively complex compared to eyeblink conditioning, and it is more difficult to connect them with specific brain regions (Simmons et al, *in preparation*). However, the goal of linking synaptic transmission with plasticity and behavior would provide much needed insight into what underlies the core symptoms of ASD. In the

cerebellum, where the circuitry is well understood relative to other brain regions, we can begin the process of elucidating the mechanisms behind the pathological behaviors observed in ASD model mice.

Materials and Methods

All procedures are in accordance with the guidelines set by the Institutional Animal Care and Use Committee of The University of Chicago.

Slice preparation: Experiments were performed on patDp/+, matDp/+, and WT mice age P35-80. Mice were anesthetized with isoflurane and decapitated. The cerebellar vermis was removed from the rest of the brain and sliced at 1ºC. Slicing was done in artificial cerebrospinal fluid (ACSF) containing the following (in mM): 124 NaCl, 5 KCl, 1.25 Na_2HPO_4, 2 $CaCl_2$, 26 $NaHCO_3$, and 10 D-glucose, bubbled with 95% O_2 and 5% CO_2. Sagittal slices of the vermis (200 μm) were cut with a vibratome (VT-1000S; Leica Microsystems). Slices incubated for at least 1 hr in oxygenated ACSF at room temperature (RT).

Somatic whole-cell patch clamp recordings: Slices were continuously perfused with ACSF during recordings. Recordings were done at RT. Whole-cell patch-clamp recordings from Purkinje cell somata (Figure 3) were performed under visual control using a 40x immersion objective mounted on a Zeiss Axioskop 2FS microscope with infrared differential interference contrast optics (Zeiss AxioCam MRm) and an EPC-10 amplifier (HEKA Electronics, Lambrecht-Pfalz, Germany). Recordings were performed in voltage-clamp or current-clamp mode when appropriate using an EPC-10 Amplifier (HEKA Electronics) and motorized

micromanipulators (Luigs & Neumann). Currents were filtered at 3 kHz, digitized at 5-10 kHz, and acquired using Patchmaster software. To record CF-EPSCs, patch pipettes (2.5-5.5 MΩ) were filled with a solution containing the following (in mM): 150 CsCl, 4.6 $MgCl_2$, 10 4-(2-hydroxyethyl)-1-piperazineethanesulfonic acid) HEPES Acid, 1 ethylene glycol-bis(β-aminoethyl ether)-N,N,N',N'-tetraacetic acid (EGTA), 0.1 $CaCl_2$, 4 adenosine triphosphate (ATP)-Na, and 0.4 guanosine triphosphate (GTP)-Na. The pH was set between 7.25-7.35 and the osmolarity was set between 295-305 mmol/kg. Purkinje cells were held at multiple potentials (-30 mV and -70 mV), and CF-EPSCs were elicited by a stimulating electrode placed in the granular layer (Figure 3). Picrotoxin (100 μM; Sigma-Aldrich, St. Louis, MO) was present in ACSF throughout all recordings. For PF-EPSCs and PF-EPSPs, a stimulating electrode was placed in the distal 2/3 of the molecular layer to avoid accidental stimulation of the CF (Figure 3), and patch pipettes (2.5-5.5 MΩ) were filled with a solution containing the following (in mM): 9 KCl, 10 KOH, 3.48 $MgCl_2$, 4 NaCl, 120 K-gluconate, 10 HEPES, 17.5 Sucrose, 4 ATP-Na, and 0.4 GTP-Na. The pH was set between 7.25-7.35, and the osmolarity was set between 295-305 mmol/kg. To measure EPSC and EPSP amplitudes, the graded increase was measured over five different stimulation intensities. The holding potential was -70 mV for PF-EPSC recordings. A train of five stimulations separated by 100 ms each was applied once every 20 s. For PF paired-pulse facilitation (PF-PPF) recordings, the stimulation intensity was adjusted so that the first PF-EPSC was between 200-300 pA. Pairs of PF-stimulations were recorded with interstimulus intervals of 10, 20, 40, and 80 ms.

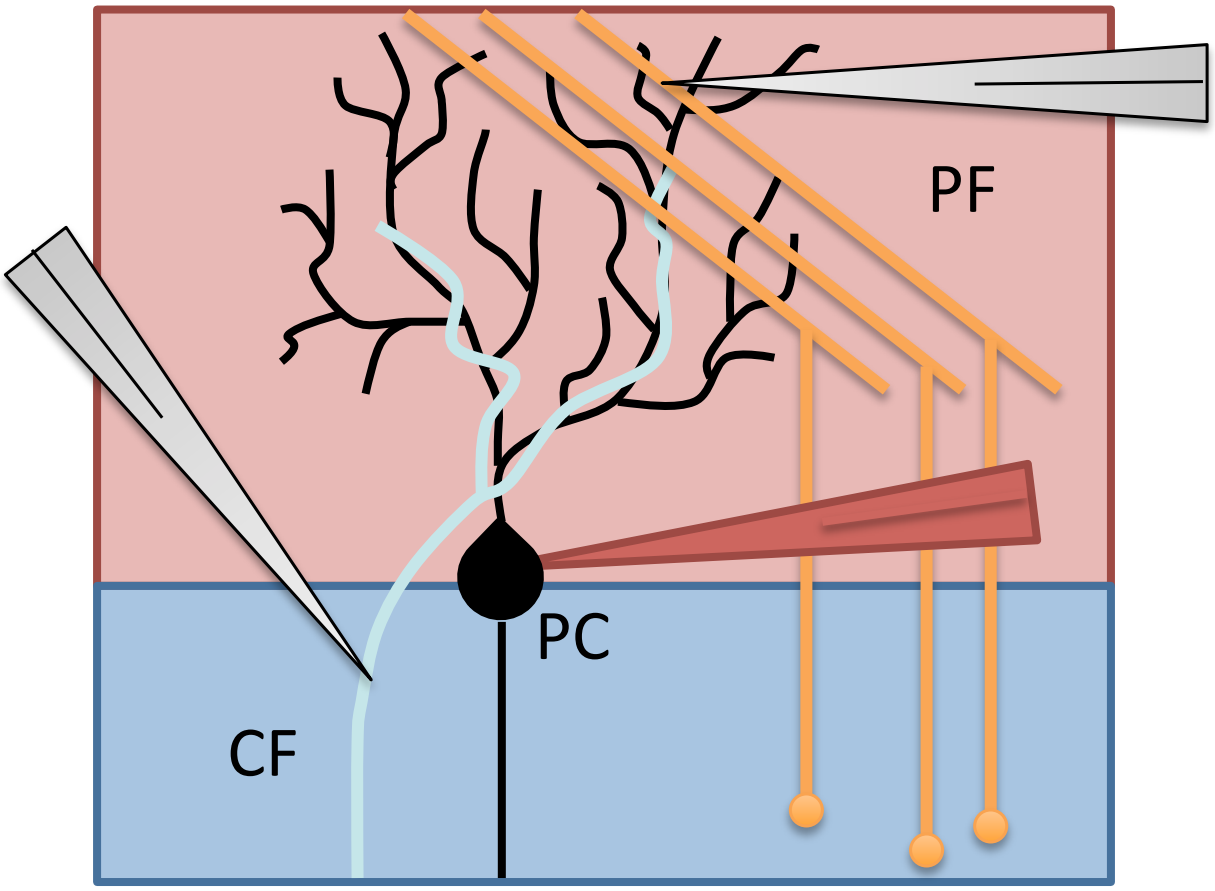

Figure 3: Patch clamp recording configuration
PC Purkinje cell, CF climbing fiber, PF parallel fibers. Red triangle indicates a somatic whole-cell patch onto a Purkinje cell. Gray triangles indicate stimulating electrodes for the PFs (top) and CF (bottom). Molecular layer in pale red, granular layer in blue. Purkinje cell in black, climbing fiber in light gray, and granule cells and parallel fibers in orange.

Immunohistochemistry: Experiments were performed on patDp/+, matDp/+, and WT mice aged 10-13 weeks. Mice were anesthetized with sterile deionized water containing 10% ketamine (Henry Schein) and 5% xylazine (Akorn), then perfused with 4% paraformaldehyde (PFA). Cerebella were removed, incubated overnight in 4% PFA, incubated for 24 hours in 30% sucrose solution, and then sliced (50 µm, sagittal) using a microtome. Permeabilization was done in deionized water containing 0.025% triton (TX) and 10% phosphate buffered saline (PBS).

Blocking was done with PBS-TX containing 10% normal donkey serum for 2 hrs. The primary antibody incubation took place overnight (rabbit anti-VGluT2, 1:500, Synaptic Systems, and mouse anti-calbindin, 1:500, Swant). The secondary antibody incubation lasted for 2 hours in the dark (donkey anti-rabbit, CY3, 1:200, Jackson ImmunoResearch, and donkey anti-mouse, AF488, 1:200, Jackson ImmunoResearch). Slices were mounted on microscope slides with Vectashied (Vector Laboratories, Inc.), held in place with coverslips, and allowed to dry overnight before visualization. Slices were imaged at 40x (Apochromat, oil immersion), and z-stacks of the molecular layer were obtained (6 images with a 0.431 μm z-step for a total height of 2.586 μm) with a confocal microscope (Zeiss LSM 5 Exciter, Axioskop 2).

Data analysis: Electrophysiological data analysis was performed using Excel (Microsoft) and Patchmaster (HEKA Electronics). Electrophysiological data were quantified using a one-way analysis of variance test (ANOVA) and post-hoc Tukey tests, or the Mann Whitney U Test when appropriate. Immunohistochemical data analysis was performed using Excel (Microsoft) and Image J (NIH). Dendrites with a diameter > 2 μm or < 2 μm were considered large caliber or fine dendrites, respectively. Colocalization of VGluT2 with calbindin was confirmed with z-stacks. VGluT2 was quantified and normalized to the measured length of large caliber and fine dendrites. Lengths between 40 μm and 85 μm were measured for primary dendrites. Data are expressed as mean ± standard error of the mean (SEM). The immunohistochemistry data were analyzed with a one-way ANOVA and post-hoc Tukey tests.

Results

To investigate the effects of delayed CF-elimination, and to determine why the 100 Hz PFb+CF LTD protocol failed to induce PF-LTD in patDp/+ mice, I tested CF-Purkinje cell synaptic transmission and PF-Purkinje cell synaptic transmission. Both the CF and the PFs are required for the LTD protocol, and I sought to determine if either showed altered signaling to Purkinje cells in patDp/+ mice compared to WT littermates. I measured CF-EPSCs in WT, patDp/+, and matDp/+ mice (Figure 4a). CF-evoked response amplitudes in Purkinje cells are enhanced in patDp/+ but not WT or matDp/+ mice (Figure 4b, EPSC1 amplitude in WT 1.36 nA ± 0.12, patDp/+ 3.19 nA ± 0.41, matDp/+ 1.65 nA ± 0.17, one-way ANOVA $p<0.0001$). The amplitudes of both EPSC1 and EPSC2 are increased in patDp/+ mice, but the paired-pulse ratio (PPR) was unaffected among the three genotypes, indicating that presynaptic release probability is unchanged (Figure 4c) and thereby is not the cause of the increase in CF-EPSC amplitudes. Instead, the enhanced CF-EPSCs in patDp/+ Purkinje cells could be the result of either a stronger postsynaptic reception of glutamate, or an increased number of presynaptic CF terminals.

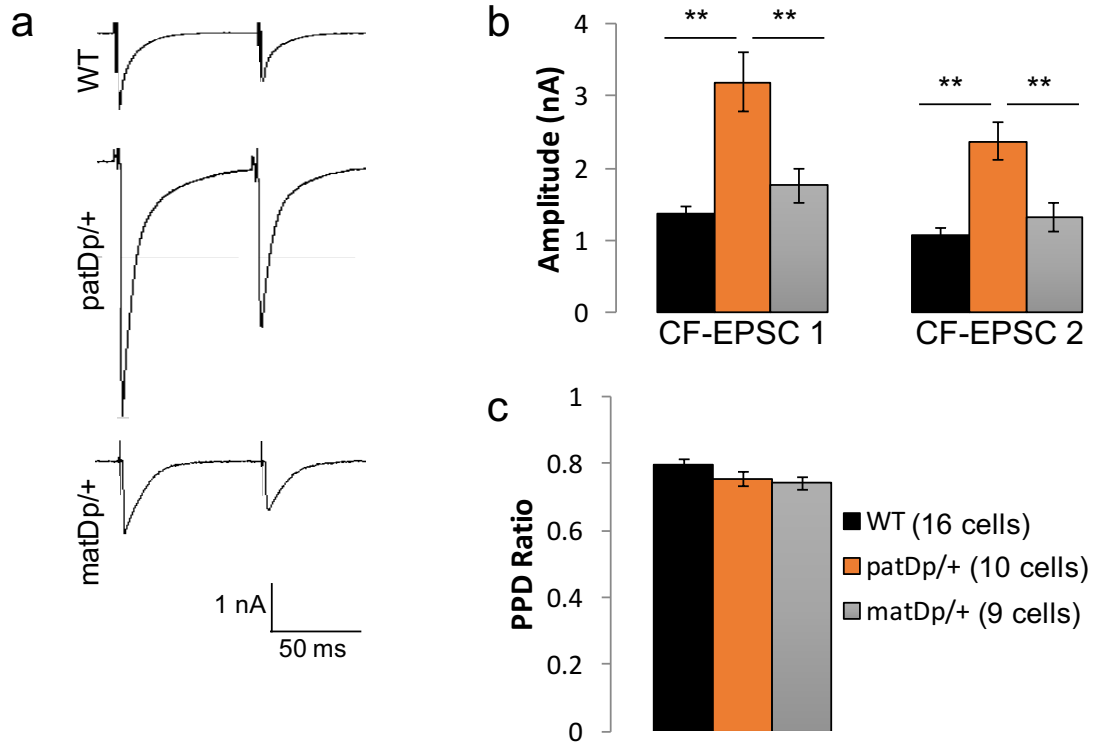

Figure 4: CF-Purkinje cell synaptic transmission is enhanced in patDp/+ mice.
a) Representative traces of CF-EPSCs in WT, patDp/+, and matDp/+ mice. b) CF-EPSC amplitudes are enhanced in patDp/+ mice compared with WT and matDp/+ mice, Tukey Test **$p<0.01$. c) The paired-pulse ratio (EPSC 2 amplitude / EPSC 1 amplitude) is comparable between WT, patDp/+, and matDp/+ mice, indicating that presynaptic release probability is unchanged.

To determine whether CFs and Purkinje cells have an increased number of synaptic connections in patDp/+ mice compared with WT mice, I performed immunohistochemistry and collected z-stacks showing cerebellar tissue with both calbindin and VGluT2 staining. Calbindin-labeling is a classical method of marking Purkinje cells because it is highly expressed in the cerebellum. Endogenous calbindin acts as a natural calcium buffer by binding calcium ions. VGluT2 staining marks the presynaptic side of CF-Purkinje cell synapses, and the presence of the glutamate transporter indicates that the synapse is functional (Figure 5a). Colocalization of calbindin and VGluT2 was confirmed by examining individual images in z-stacks. Though

infrequent, any "floating" VGluT2 spots were considered non-specific staining, and thus were not counted. The data reveal that indeed there is an increased density of CF-Purkinje cell synapses in patDp/+ mice both on large caliber dendrites (>2 µm diameter, Figure 5b, WT: 18.98 ± 1.24, patDp/+: 25.31 ± 1.17, matDp/+: 17.82 ± 0.99, one-way ANOVA p=0.0007) and on fine dendrites (<2 µm diameter, Figure 5c, WT: 3.88 ± 0.49, patDp/+ 7.71 ± 0.68, matDp/+ 4.66 ± 0.54, one-way ANOVA p=0.0006). Measured dendritic lengths were not significantly different between the genotypes. The increase in VGluT2 density on the fine dendrites in patDp/+ mice is particularly notable because CF-Purkinje cell synapses are rarely found on fine dendrites (WT vs. patDp/+ post-hoc Tukey test p=0.0009). Typically, the fine dendrites are where PFs make synaptic connections with Purkinje cells.

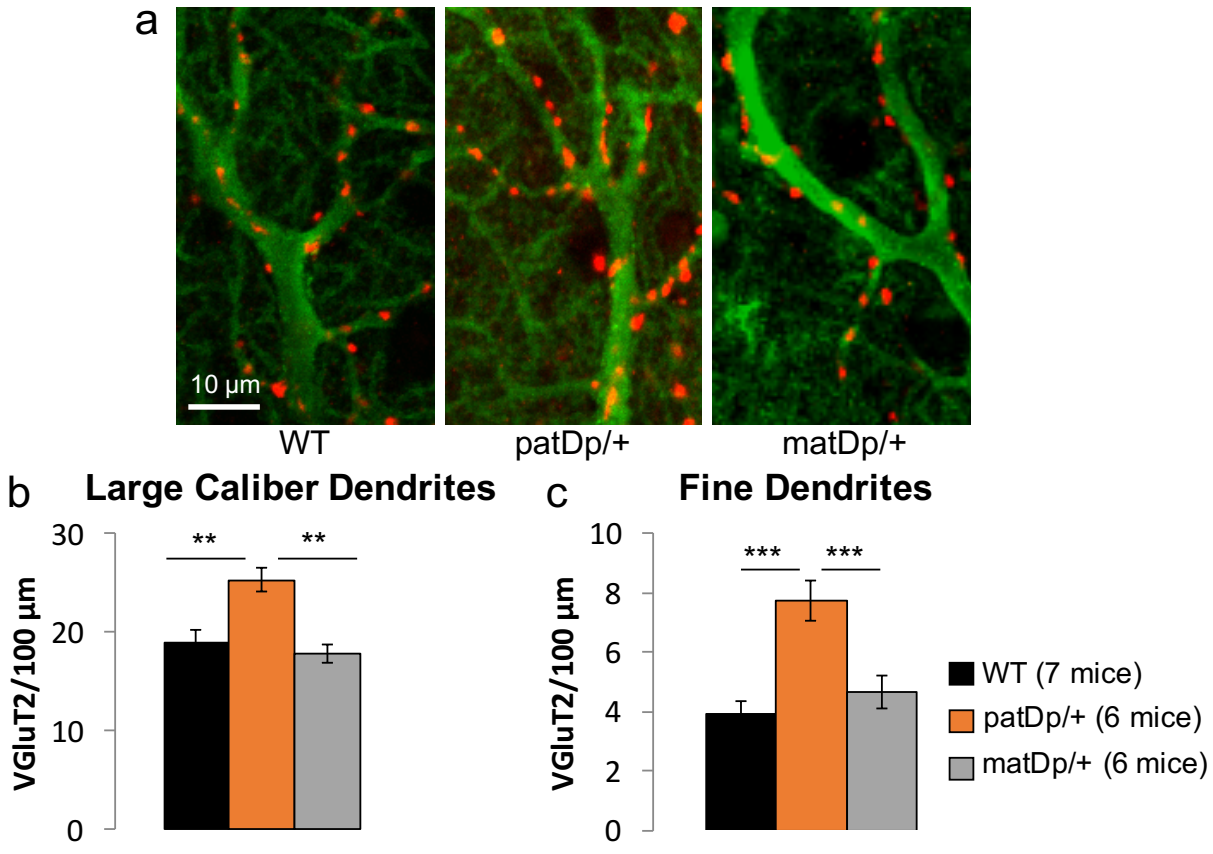

Figure 5: CF-Purkinje cell synaptic density is enhanced in patDp/+ mice.

Figure 5, continued. CF-Purkinje cell synaptic density is enhanced in patDp/+ mice.
The number of CF-Purkinje cell synapses per 100 μm on both large caliber and fine dendrites is enhanced in patDp/+ mice, but not matDp/+ mice (aged 10-13 weeks). This enhancement of CF-Purkinje cell synapses may result from faulty CF-elimination during development. In patDp/+ mice, a CF forms ectopic synapses on fine dendrites, which are considered to be areas mainly for PF-Purkinje cell synapses in WT mice. a) Immunohistochemistry showing both large caliber and fine dendrites in sagittal cerebellar sections for WT (left), patDp/+ (center), and matDp/+ (right). Red: VGluT2 marks CF-Purkinje cell synapses. Green: calbindin is a Purkinje cell marker. Scale bar = 10 μm. b) Increased staining of VGluT2 per 100 μm of large caliber dendrites indicates enhanced levels of CF-Purkinje cell synapses in patDp/+ mice compared with WT and matDp/+ mice. c) Increased VGluT2 staining per 100 μm of fine dendrites reveals ectopic CF-Purkinje cell synapses in territory typically reserved for PF-Purkinje cell synapses. Enhanced ectopic CF-Purkinje cell synapses are observed in patDp/+ mice compared with WT and matDp/+ mice. Post-hoc Tukey Tests, **$p<0.01$, ***$p<0.001$.

After finding that CFs make ectopic synapses onto the fine dendrites of Purkinje cells in patDp/+ mice, I predicted that PFs would be weakly connected with Purkinje cells since the CF had invaded their territory. Recording PF-EPSPs from patch-clamped Purkinje cells using 5 PF stimulations at 10 Hz every 20 seconds (Figure 6a) revealed two things 1) by the fifth EPSP in the train, PF-EPSP amplitudes are decreased in patDp/+ mice compared with WT mice (Figure 6b, WT: 17.38 mV ± 3.92, patDp/+ 8.31 mV ± 1.70, Mann Whitney Test $p = 0.03$), and 2) EPSPs recorded from Purkinje cells in patDp/+ mice have a lower probability of reaching spike threshold and generating an action potential than EPSPs recorded from WT littermates (Figure 6c, EPSP2 WT: 0.93 ± 0.22, patDp/+: 0.26 ± 0.12, Mann Whitney test $p=0.0214$; EPSP3 WT: 1.04 ± 0.22, patDp/+: 0.22 ± 0.11, $p=0.0131$; EPSP4 WT: 1.07 ± 0.22, patDp/+: 0.19 ± 0.10, $p=0.0105$; EPSP5 WT: 1.02 ± 0.23, patDp/+: 0.18 ± 0.10, $p=0.0093$). Finding that basic synaptic transmission is impaired at PF-Purkinje cells in patDp/+ mice, I predicted that the PF-PPF might also be abnormal. To measure any abnormalities, the PF-PPF (EPSC2 amplitude / EPSC1 amplitude) for two PF-EPSCs separated by different interstimulus intervals, beginning with 10 ms (Figure 6d), was calculated. The changes in PF-PPF follow the rules of spike timing-dependent plasticity in that more facilitation occurs at shorter interstimulus intervals than at

longer interstimulus intervals (Figure 6e). The differences in PF-PPF between WT and patDp/+ mice are statistically significant at shorter interstimulus intervals, including 10 ms (WT: 2.81 ± 0.13, patDp/+ 2.35 ± 0.12, Mann Whitney Test p=0.0091) and 20 ms (WT: 2.70 ± 0.12, patDp/+ 2.36 ± 0.08, Mann Whitney Test p=0.0332). The decreased facilitation displayed in pairs of PF-EPSCs from patDp/+ mice at an interstimulus interval of 10 ms is especially notable because the PF-LTD protocol Piochon and colleagues used includes a burst of PF pulses that are separated by 10 ms each (Piochon et al 2014). The deficiency in facilitation shown by PF-EPSCs in patDp/+ mice suggests an impairment in the ability to buildup calcium as a result of repeated, high-frequency PF pulses. Furthermore, such a deficiency suggests that the calcium that is accumulated during the PFb portion of the 100 Hz PFb+CF induction protocol is insufficient to induce PF-LTD.

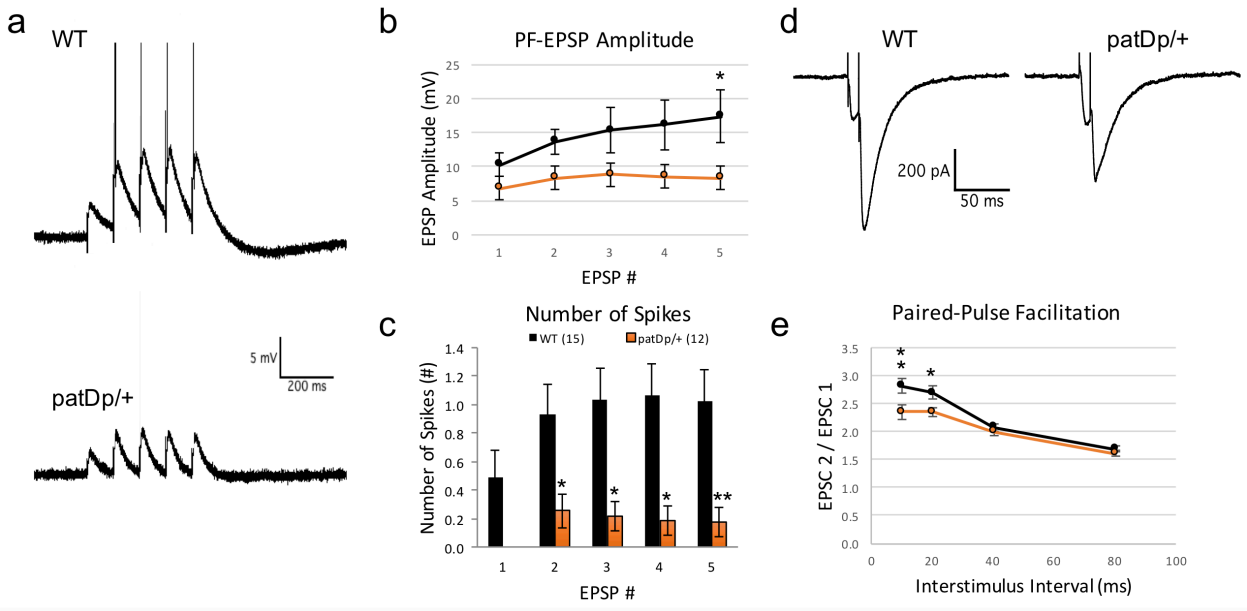

Figure 6: PF-Purkinje cell synaptic transmission and buildup are weakened in patDp/+ mice. a) Typical traces from WT (top) and patDp/+ (bottom) of a train of 5 PF-EPSPs at 10 Hz. b) Average amplitudes of WT (n=15) and patDp/+ (n=12) PF-EPSPs. Mixed-ANOVA p=0.0026, Mann Whitney Test p=0.03 for fifth EPSP. c) The average number of spikes on each EPSP in the train of 5 EPSPs. d) Typical traces from WT and patDp/+ PF-EPSPs with a paired pulse interval of 10 ms. e) Average paired pulse facilitation ratio of PF-EPSP amplitudes in Purkinje cells from WT and patDp/+ mice at interstimulus intervals of 10, 20, 40, and 80 ms. For 10 ms,

Figure 6, continued. WT (n=23) and patDp/+ (n=24). For 20, 40, and 80 ms, WT (n=24) and patDp/+ (n=24). Mann Whitney Test, *p<0.05, **p<0.01

Discussion

When examining motor symptoms associated with ASD, it is helpful to get an understanding of what underlies them in order to fully understand how they arise. One way to examine the mechanisms behind impaired motor behavior and cerebellar synaptic plasticity is to observe and manipulate the basic components of the cerebellar circuit. The excitatory inputs to Purkinje cells, the CF and PFs, must be functionally intact in order for the corresponding plasticity mechanisms and behaviors to remain unaffected.

The findings that CF-EPSCs show enhanced amplitudes in patDp/+ mice, and that CFs make ectopic synapses onto Purkinje cells, indicate that CF input to Purkinje cells is strengthened to a pathological level. Synaptic pathology affects not only the adult state of the circuit, but it also profoundly affects cerebellar development. It has been documented that CF-elimination is delayed in patDp/+ mice compared to WT littermates (Piochon et al 2014). The persistence of multiple CFs on Purkinje cells in patDp/+ mice is lasting evidence of impaired elimination. It is likely that the CFs take up a great deal of space making synapses along Purkinje cell dendrites – including the fine dendrites. Typically, the fine dendrites are sites for PF-Purkinje cell synapses. However, in the patDp/+ mice, it appears that either 1) the CF is overgrown and takes dendritic "real estate" away from PFs, or 2) the PF inputs are weak and underdeveloped, leaving extra empty space for the CF to invade.

Whether CFs invade the PF territory of the fine Purkinje cell dendrites first, or whether the CFs simply fill in empty sections of Purkinje cell dendrites where PFs have failed to make synapses can be determined by immunostaining for VGluT1 and VGluT2 at different points during development, and measuring how the territories of PFs and the CF in the molecular layer

change. In the past, evidence has shown that when PFs are selectively weakened during development, the CF does indeed expand into what may normally be considered PF-territory (Crépel et al 1980, Kano et al 1998, Kurihara et al 1997, Hirai et al 2005, Watanabe 2008, review: Cesa & Strata 2009).

It has been noted several times that the balance between excitatory glutamatergic and inhibitory γ-aminobutyric acid- (GABA)ergic synaptic transmission is altered in ASD in brain regions including the neocortex, hippocampus, amygdala, and cerebellum (review: Uzunova et al 2016). This lack of controlled balance between excitatory and inhibitory transmission is thought to underlie motor deficits, sensory abnormalities, cognitive alterations, and the presentation of seizures, depending on the respective brain regions affected. Although inhibitory signaling through $GABA_A$ receptors has been blocked in these experiments by adding picrotoxin to the ACSF, there is nonetheless an imbalance of inputs to Purkinje cells in patDp/+ mice. This imbalance is not excitatory/inhibitory, but rather it is excitatory/excitatory. Different regions of Purkinje cell dendrites typically receive excitatory signals from particular inputs. In patDp/+ mice, the territory and strength of these inputs has changed such that CFs produce enhanced synaptic signals and the PFs produce weakened synaptic signals. This has profound effects on development that may last throughout life, and has impaired synaptic plasticity which underlies important learning mechanisms for behaviors. Since the 15q11-13 duplicated chromosomal region contains genes for several GABA receptor subunits (Figure 1), it will be useful to perform experiments in the absence of picrotoxin in order to measure any altered inhibitory synaptic transmission between interneurons and Purkinje cells.

While Piochon and colleagues hypothesized that PF-LTD was impaired in patDp/+ mice because the strong CF signal reached a sort of ceiling limit, or saturated signal (Piochon et al

2014), new results indicate that despite the strong CF signal, the PFs in patDp/+ mice are weakened, and are quite possibly too weak to induce PF-LTD. PF synaptic transmission was measured in two ways: 1) PF-EPSP amplitudes in a train of 5 stimulations, and 2) the PF-PPF ratio. The first measurement showed that PF-EPSP amplitudes are reduced in patDp/+ mice compared to WT mice, and supports the idea that basic PF-Purkinje cell synaptic transmission is weakened. This low frequency (10 Hz) group of 5 stimulations shows lower amplitudes, but also indicates less buildup as the train of stimulations progresses. The second measurement addresses the appearance of decreased calcium buildup by showing that PF-PPF is decreased in patDp/+ mice compared to WT littermates. This suggests either that Purkinje cells in patDp/+ mice respond less to PF stimulations, or that there is less residual calcium in the presynaptic PF terminals in patDp/+ mice to help enhance a second PF-EPSP. Typically, the PF-Purkinje cell synapse in WT mice has residual calcium left over in the presynaptic terminal after firing. In accordance with short term plasticity, this residual calcium increases the strength of a second EPSP if it is close enough in time.

In future studies, it may be useful to explore potential alterations to presynaptic release probability (by examining mini EPSCs) to further understand the source of the weakened PF synaptic transmission and buildup. Furthermore, spine calcium imaging on fine dendrites of Purkinje cells can be used to screen for alterations to the sensitivity of the postsynaptic half of the synapse. If there are impairments to the sensitivity of Purkinje cells in receiving inputs, it may additionally be useful to look for differences in spike thresholds and to examine whether intrinsic plasticity can be induced in a similar manner in WT and patDp/+ mice.

Chapter 3: Calcium Signaling and Synaptic Plasticity in Purkinje Cell Dendritic Spines in 15q11-13 Mice

Introduction

Two major forms of synaptic plasticity, LTD and LTP, can and do take place at the same synapses, and can act as reversal mechanisms for each other (Sakuri 1987, Sakuri 1990, Hirano 1990, Crépel & Jaillard 1991, Shibuki & Okada 1992, Jörntell & Hansel 2006). Whether a PF-Purkinje cell synapse potentiates or depresses, regardless of the PF stimulation frequency (Piochon et al 2016), depends on the co-activation of the PFs with the CF, the latter of which initiates large postsynaptic calcium transients (Sakuri 1990, Konnerth et al 1992, Augustine et al 2003). A CF induces a large depolarization event in a Purkinje cell. First AMPA receptors open and allow depolarization, then voltage-gated calcium channels open and allow even greater depolarization, and finally the Mg^{2+} block on NMDA receptors is removed and the NMDA receptors open and allow the influx of sodium and calcium ions into the Purkinje cell. In the cerebellum, this strong influx of calcium through NMDA receptors is required for PF-LTD rather than PF-LTP (Coesmans et al 2004). It is important to note that this is in contrast to the calcium thresholds for bidirectional synaptic plasticity at synapses between excitatory inputs to hippocampal and neocortical pyramidal cells (Bienenstock et al 1982, Bear et al 1987, Artola et al 1990, Hansel et al 1997).

Calcium signals that passed through spines on higher order Purkinje cell dendrites in response to PF and CF stimulations were measured in order to examine why PF-LTD is impaired in patDp/+ mice. I hypothesized that a portion of the cerebellar circuit provided abnormal levels of calcium to Purkinje cells – either that the CF provided enhanced calcium signaling, or that the PFs provided insufficient calcium signaling – to successfully induce LTD at the PF-Purkinje cell

synapse. By monitoring calcium transients during three different tetanization protocols including LTD induction (100 Hz PFb+CF), the CF alone (CF), and the PFs alone which is also the LTP induction protocol (100 Hz PFb), it was indeed revealed that the PFb-evoked calcium transient is significantly weaker in patDp/+ mice than it is in WT and matDp/+ mice. It is likely that this diminished PFb-evoked calcium signal in patDp/+ mice is too weak to induce PF-LTD.

One way to test the prediction that PFb-evoked calcium signaling is insufficient to induce PF-LTD is to increase the calcium influx to Purkinje cells. Calcium influx was experimentally increased pharmacologically by supplementing the ACSF with 300 μM CX546 in an effort to restore LTD at the PF-Purkinje cell synapse in patDp/+ mice. CX546 is a pharmacological reagent that promotes depolarization by allosterically modulating AMPA receptors to slow desensitization and deactivation (Arai & Kessler 2007). In the presence of CX546, AMPA receptors remain open longer than usual, which allows for extra Na^+ influx, and in doing so, increases depolarization enough to open NMDA receptors as well as voltage-gated calcium channels. In this way, the experimental use of CX546 manipulates the circuitry so that more calcium than normal enters postsynaptic Purkinje cells (van Beugen et al 2014). Additionally, CX546 is known to increase presynaptic release probability, and has been shown to promote LTP in the hippocampus (Chang et al 2014). Importantly, CX546 has previously been used successfully to restore PF-LTD in the cerebellum by enhancing postsynaptic calcium transients. In the research presented in this chapter, the addition of CX546 to the ACSF does indeed restore PF-LTD in patDp/+ mice to levels seen in WT littermates, as predicted.

Materials and Methods

All procedures are in accordance with the guidelines set by the Institutional Animal Care and Use Committee of the University of Chicago.

Slice preparation: Sagittal cerebellar slices (200 μm, vermis) were prepared (as described in Chapter 2 Methods) from 4-7-week-old WT, patDp/+, and matDp/+ mice. Slices incubated at RT in ACSF containing the following (in mM): 124 NaCl, 5 KCl, 1.25 Na_2HPO_4, 2 $CaCl_2$, 26 $NaHCO_3$, and 10 D-glucose, bubbled with 95% O_2 and 5% CO_2, and supplemented with 100 μM picrotoxin (Sigma).

Somatic whole-cell patch clamp recordings: Purkinje cells were patched at RT under visual control using motorized micromanipulators (Luigs & Neumann) and a 63x Apochromat water immersion objective on a Zeiss LSM 5 Exciter microscope. Recordings were performed in voltage-clamp or current-clamp mode using an EPC-10 amplifier (HEKA Electronics). Whole-cell somatic patch clamp recordings were made using electrodes in glass pipettes (2.5-5.5 MΩ) containing the following (in mM): 9 KCl, 10 KOH, 3.48 $MgCl_2$, 4 NaCl, 120 K-gluconate, 10 HEPES, 17.5 Sucrose, 4 ATP-Na, and 0.4 GTP-Na. The pH was set between 7.25-7.35, and the osmolarity was set between 295-305 mmol/kg. For calcium imaging experiments, the patch pipette also contained 300 μM Fluo-5F and 30 μM Alexa 633. A stimulating electrode was placed in the granular layer to excite the CF, and a second simulating electrode was place in the upper 2/3 of the molecular layer to excite the PFs. The holding potential was -70 mV.

Calcium imaging: Calcium imaging experiments were performed in patDp/+, matDp/+, and WT mice between the ages of 4-6 weeks. Patch-clamped Purkinje cells were loaded simultaneously with red fluorescence (R) calcium-insensitive dye (Alexa 633, 30 μM, Invitrogen) and green fluorescence (G) calcium-sensitive dye (Fluo-5F, 300 μM, Invitrogen). The green fluorescence was excited at 488 nm using an argon laser (Lasos Lasertechnik), and the red fluorescence was excited at 633 nm by a helium-neon laser (Lasos Lasertechnik). Calcium transients were recorded using a Zeiss LSM 5 Exciter confocal microscope equipped with a 63x Apochromat water objective. To evoke calcium transients, three stimulation protocols were used: 100 Hz PFb, single CF, and 100 Hz PFb+CF where the CF is stimulated 100 ms after the first (of eight) PF stimulations in the PFb. Calcium transients were calculated as $\Delta G/R=(G(_t)-G_0)/R$ in dendritic spines that responded maximally to synaptic activation.

Synaptic plasticity: Patch-clamped Purkinje cells from mice aged 4-7 weeks were held at -70 mV. Baseline PF-EPSCs were recorded (200 to 300 pA). Tetanization consisted of a burst of 8 PF stimulations at 100 Hz (PFb) plus one CF stimulation 100 ms after the onset of the PFb. This tetanization was repeated at 1 Hz for 5 min. Following tetanization, PF-EPSC amplitudes were measured for 30 minutes. Cells were included in final analyses only if their series resistance and input resistance were stable ± 15% of the corresponding resistances measured during the baseline. ACSF was supplemented with 300 μM CX546 (Sigma) in the rescue group.

Data analysis: Calcium transients were measured using Zen 2008 software (Carl Zeiss MicroImaging), Excel (Microsoft), and Patchmaster (HEKA Electronics). Transients were analyzed using a one-way ANOVA and post-hoc Tukey tests. Synaptic plasticity data were

measured using Patchmaster and analyzed in Excel. EPSC amplitudes were analyzed using t-tests to quantify the difference from the baseline amplitude within a single group, and Mann Whitney U Tests between groups. EPSC amplitudes were normalized to their baseline levels, which were between 200-300 pA for all genotypes.

Results

CFs and Purkinje cells in patDp/+ mice have an increased density of synaptic connections on both large caliber and fine dendrites, which could lead to the observed enhanced amplitudes of CF-EPSCs (Figure 4b). However, the question of whether there is increased strength in the reception of CF signals to Purkinje cells remained to be explored. In order to investigate whether CF-evoked activation of Purkinje cells produces a different amount of calcium influx in patDp/+ mice, calcium signaling in Purkinje cell spines was measured (Figure 7a). Spines are critical to examine because they contain PF-Purkinje cell synapses, which are the sites of PF-LTD. It is important to note that PF-LTD requires the activation of both PFs and the CF (Coesmans et al 2004, Piochon et al 2010, Schonewille et al 2010, Ito M et al 2014), and requires more postsynaptic calcium influx than PF-LTP (Coesmans et al 2004).

Three different stimulation protocols were applied to each patch-clamped cell: 100 Hz PFb+CF (PF-LTD induction protocol), single CF pulse, and 100 Hz PFb (PF-LTP induction protocol, Figure 7b) and their respective, simultaneous calcium signals were obtained (Figure 7c). The three protocols were applied in random order, to avoid any potential effects of order, and were later averaged together over all cells in each genotype (Figure 7d). Calcium transient amplitudes were quantified from the beginning of the stimulus onset until 200 ms later in order to capture the majority of the transient (Figure 7e). For the 100 Hz PFb+CF protocol and the 100

Hz PFb protocol, a lower amplitude calcium transient (as measured by change in calcium sensitive fluorescence / baseline fluorescence, (ΔG/R)) was measured in spines from Purkinje cells in patDp/+ mice compared with those from WT and matDp/+ mice (PFb+CF: WT = 0.654 ± 0.098, patDp/+ = 0.286 ± 0.056, matDp/+ = 0.727 ± 0.177, Kruskal Wallis Test p = 0.0127; PFb: WT = 0.425 ± 0.069, patDp/+ = 0.145 ± 0.038, matDp/+ = 0.319 ± 0.083, Kruskal Wallis Test p = 0.0024). There was no change in CF-evoked calcium transients between the genotypes (CF: WT = 0.155 ± 0.026, patDp/+ = 0.141 ± 0.027, matDp/+ = 0.129 ± 0.027, Kruskal Wallis Test p = 0.6942). The weak PFb-induced calcium transient in patDp/+ mice compared with WT and matDp/+ mice suggests that PFs in patDp/+ mice provide very weak input to Purkinje cells. It is highly likely that this weak PF input does not provide sufficient calcium influx to Purkinje cells to induce PF-LTD during the 100 Hz PFb+CF LTD protocol.

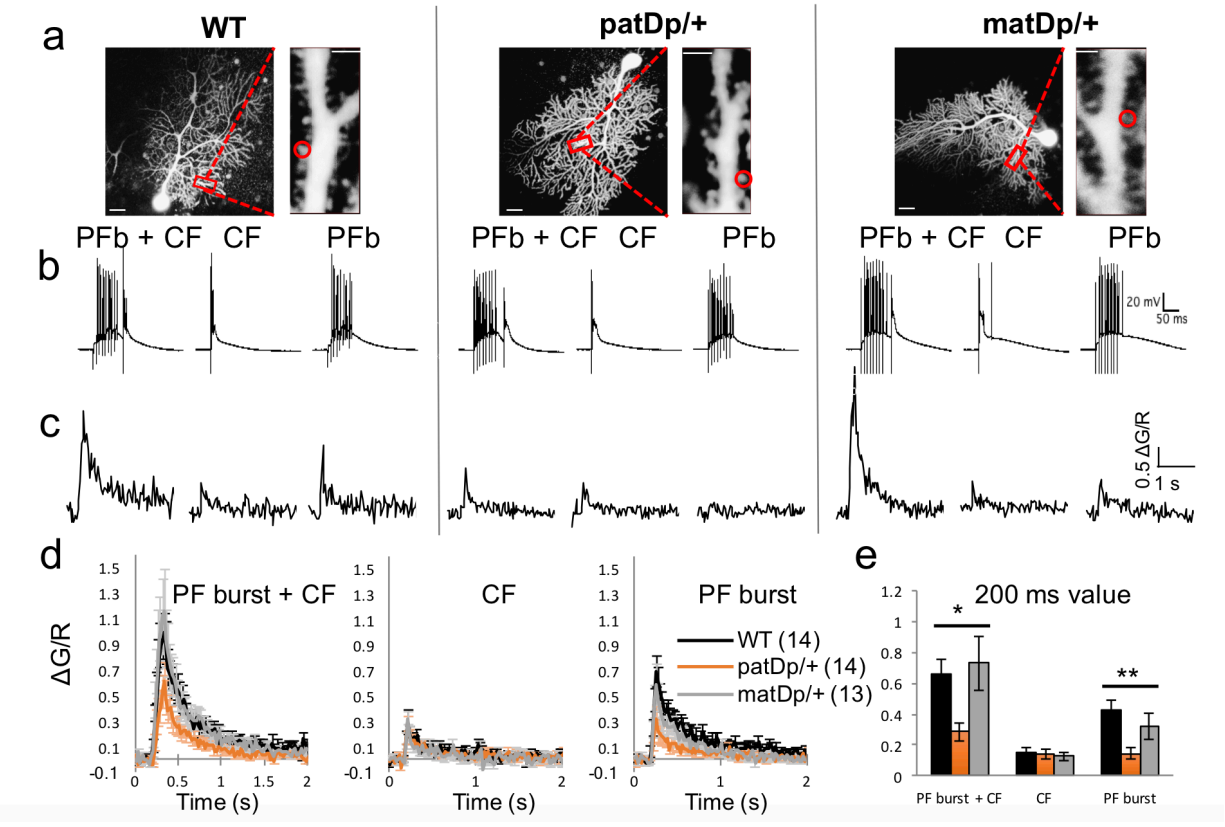

Figure 7: PF-evoked calcium transients are decreased in spines from patDp/+ mice.

Figure 7, continued. PF-evoked calcium transients are decreased in spines from patDp/+ mice. a) Representative images of WT (left), patDp/+ (middle), and matDp/+ (right) Purkinje cells filled with Fluo-5F and Alexa633 dye. Red box indicates the dendrite with the maximally responding spine, magnified to the right of each Purkinje cell image. Red circle indicates the maximally responding spine. Scale bar = 20 μm. b) Electrophysiological responses (from somatic whole-cell patches) to the following stimuli: 100 Hz PFb + CF, CF alone, and 100 Hz PFb. c) Simultaneously recorded dendritic spine calcium transients in the maximally responding Purkinje cell spine. d) Average of all calcium transients for the three stimulation protocols in all recorded Purkinje cell spines. e) Quantification of calcium signal amplitudes during a 200 ms window that begins at stimulus onset. Amplitudes are reduced in calcium transients involving PFs. Kruskal Wallis Test *$p<0.05$, **$p<0.01$.

We successfully replicated the result from previously published studies showing that 100 Hz PFb+CF stimulation at 1 Hz for 5 minutes induces PF-LTD in Purkinje cells in WT mice, but leads to potentiation of EPSCs in patDp/+ mice (Piochon et al 2014, patDp/+ difference from baseline at 25-30 min post-tetanization 149.737% ± 10.468, t-test $p = 0.003$). To confirm whether insufficient calcium influx to Purkinje cells contributed to the failure of the PF-LTD protocol at PF-Purkinje cell synapses in patDp/+ mice, we used CX546 to indirectly increase the influx. CX546 is an ampakine that allosterically modulates AMPA receptors to keep them open for more time than normal. When the AMPA receptors are open longer, more sodium enters Purkinje cells, promoting depolarization. Increased depolarization removes the Mg^{2+} block from NMDA receptors, allowing them to open, further promoting depolarization and opening voltage-gated calcium channels. Opening the voltage-gated calcium channels increases calcium influx to Purkinje cells. Representative traces of PF-evoked EPSCs before and after tetanization show successful PF-LTD in WT and patDp/+ CX546 mice, but potentiation in patDp/+ mice without CX546 (Figure 8a). In the presence of ACSF supplemented with 300 μm CX546, and found that PF-LTD was restored to WT levels at PF-Purkinje cell synapses in patDp/+ mice (Figure 8b, difference from baseline at 25-30 min post-tetanization, WT: 72.225% ± 2.571, t-test 0.0004; patDp/+ CX546: 73.738% ± 5.721, t-test $p = 0.006$; difference between genotypes: WT vs.

patDp/+ vs. patDp/+ CX546 at 25-30 min post-tetanization, Kruskal Wallis Test p = 0.002). This successful restoration of PF-LTD indicates that inputs to Purkinje cells in patDp/+ mice do indeed provide insufficient calcium influx to induce PF-LTD in regular ACSF.

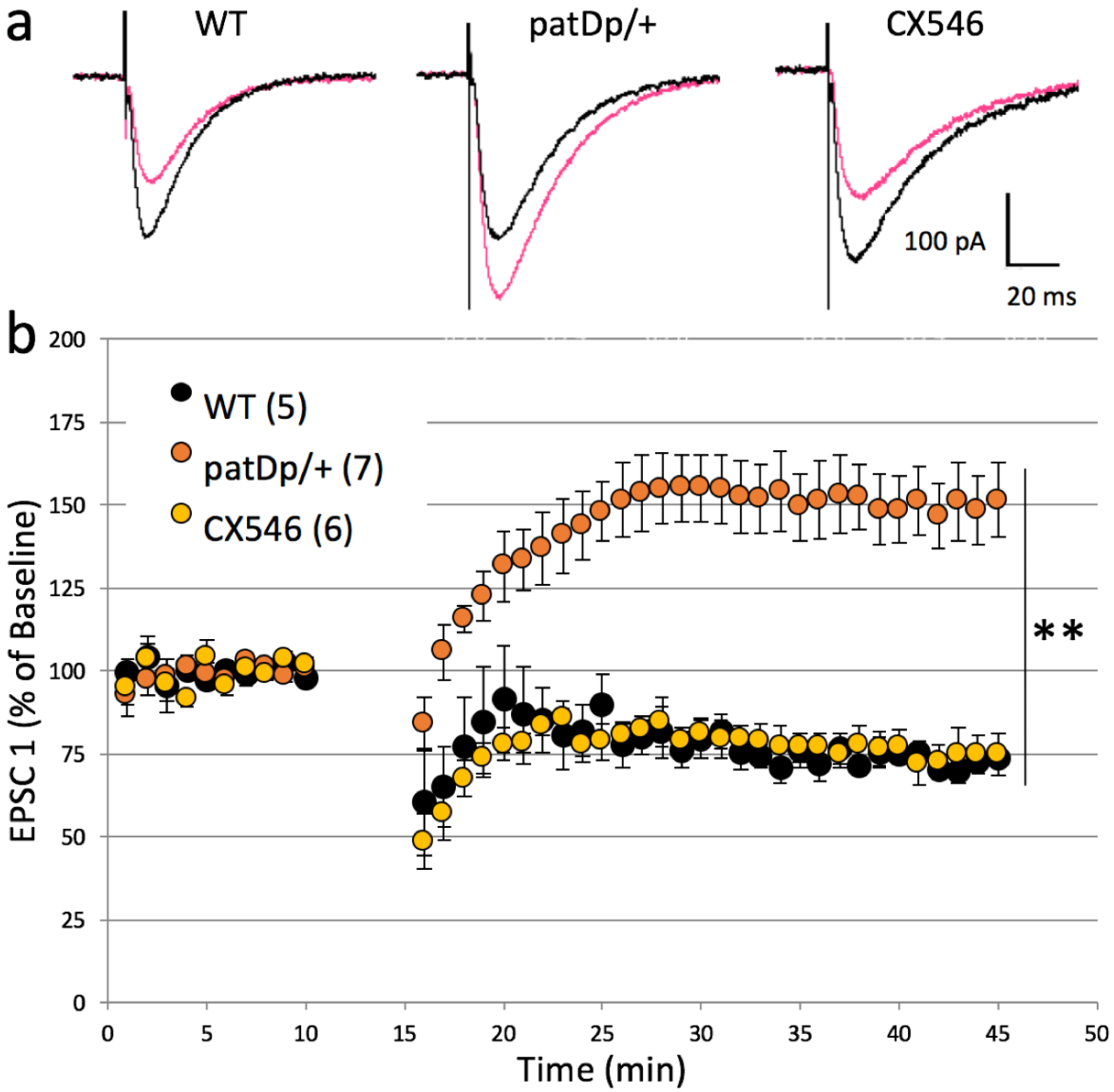

Figure 8: PF-LTD is impaired in patDp/+ mice, but restored with CX546.
Tetanization protocol: A PFb (8 pulses at 100 Hz) is applied by a stimulation electrode in the upper 2/3 of the molecular layer. The CF input is activated by a second stimulation electrode in the granular layer 100 ms after the onset of the PF stimulus. Tetanization begins at t = 10 min and continues for 5 min. a) Typical PF-EPSCs from WT, patDp/+, and patDp/+ CX546 experiments. Black: pre-tetanization. Pink: post-tetanization. b) Time graph showing LTD at PF-Purkinje cell synapses in WT mice and potentiation from the same 100 Hz PFb+CF

Figure 8, continued. tetanization protocol in patDp/+ mice. When the ACSF is supplemented with CX546, PF-LTD is restored in patDp/+ mice. Error bars indicate SEM. Kruskal Wallis Test, **p<0.01.

Discussion

Initially, it was predicted that calcium transients initiated by CF-evoked stimulations would be larger in patDp/+ mice than in WT and matDp/+ mice because CF-EPSCs are enhanced in patDp/+ mice, and CFs provide a large excitation of calcium influx to Purkinje cells. However, CF-evoked calcium transients measured in Purkinje cell spines were not different in patDp/+ mice. It is possible that a potential difference in CF-evoked calcium transients is obscured by the limits of the spine calcium imaging technique. Specifically, spines are where PFs make synapses onto Purkinje cells, but CFs mainly make synapses on large caliber dendrites that are smooth and have very few spines. Much of the CF-evoked calcium transient and regenerative CF signal reverberates around the Purkinje cell soma and large caliber dendrites. In order to get a more accurate measure of CF-evoked calcium signals, a more appropriate region of interest to examine would be larger caliber dendrites. Imaging large dendrites, however, poses challenges related to phototoxicity from prolonged exposure since the time required to image a wider dendrite is longer than the time required to image a thinner dendrite. Spine calcium imaging in the distal dendrites is perhaps best suited for measuring PF-evoked calcium transients.

Spine calcium imaging during a PFb as well as a PFb+CF shows weak calcium signaling into Purkinje cells in patDp/+ mice. This weak calcium signaling supports the hypothesis that PF synaptic transmission is insufficient to induce LTD. To further test whether or not a lack of calcium prevented the induction of PF-LTD during the 100 Hz PFb+CF protocol, we decided to increase the calcium influx to Purkinje cells experimentally. There are many ways to increase

extracellular calcium including adding a higher concentration of calcium to the ACSF bath, and using pharmacological manipulation. We chose to supplement the ACSF with CX546, which is an ampakine that promotes postsynaptic depolarization by allosterically modulating AMPA receptors. As such, CX546 increases the calcium influx into postsynaptic Purkinje cells in response to electrical stimulation. Indeed, the addition of CX546 successfully rescued the impaired PF-LTD in patDp/+ mice. Rescue by the addition of CX546, which acts by increasing calcium influx, supports the prediction that the calcium signaling in patDp/+ mice between PFs and Purkinje cells is too weak to induce PF-LTD.

In future studies, it would be interesting to test whether the addition of CX546 could also restore alterations to basic synaptic transmission observed in PF-EPSPs (Figure 6b, c). Moreover, it could potentially be important to consider therapeutic effects of ampakines for use during development to mediate balanced development of brain circuits. If an ampakine, or other compound, could boost PF strength during development and help maintain it throughout life, then it is possible that impairments to synaptic plasticity and behaviors could be ameliorated or minimized.

Chapter 4: UBE3A and CYFIP1 as Candidate Genes for ASD Pathology

Introduction

One major goal in biological research is to associate genes with specific behaviors or traits. In order to better understand ASD symptoms displayed by patients and the autistic-like symptoms displayed by patDp/+ mice, I sought to determine which gene(s) in the 15q11-13 duplication showed altered expression levels. The region encompasses approximately 20 different genes, depending on where the breakpoints are during each duplication. In human patients, some of the genes are maternally expressed, some are paternally expressed, and others are non-imprinting (Nakatani et al 2009). However, the inheritance pattern of the individual genes in this region is up for questioning because the general imprinting pattern in the mouse model is the opposite of what is seen in patients. In humans, patients bearing a maternal duplication show ASD symptoms, but in mice, patDp/+ individuals show autism-like symptoms (Cook & Scherer 2008, Nakatani et al 2009, Urraca et al 2013). Because of this poorly understood inheritance pattern, there are many genes of interest to be studied in the 15q11-13 chromosomal segment, including several GABA receptors, CYFIP1, and UBE3A.

UBE3A is an E3 ubiquitin-protein ligase (also known as E6-AP) that ubiquitinates proteins, targeting them to the lysosome for degradation. In Purkinje cells, UBE3A is highly expressed and is found at synapses and in the nucleus (Dindot et al 2008). UBE3A is of interest for further study because it has downstream targets at synapses such as Arc, which is highly involved in synaptic plasticity and synaptic pruning (Greer et al 2010, Kühnle et al 2013), two cellular processes that have similar molecular pathways (review: Piochon et al 2016, Hansel 2018). Furthermore, UBE3A has already been linked to multiple pathologies. It is well-known that human offspring receiving a deletion (in contrast to a duplication) of UBE3A maternally will

be afflicted with Angelman syndrome, and offspring with a paternal deletion of UBE3A will be afflicted with Prader-Willi syndrome (Albrecht et al 1997, Dindot et al 2008, Heck et al 2008). The connection between a deletion of UBE3A and these two syndromes is well established, suggesting that a precise or tightly controlled level of UBE3A may be critical for typical development. Moreover, recent research has shown that overexpression of UBE3A in mice linearly correlates with autism-like symptoms such as severity of social impairments, and increases in the amount of time spent participating in perseverative behaviors, as well as impaired glutamatergic synaptic transmission in cortical pyramidal neurons in the barrel cortex (Smith et al 2011). Furthermore, increases in the expression of Ube3a have been associated with decreased levels of cerebellin-1 (Cbln1) protein (Krishnan et al 2017). Cbln1 forms a complex across the PF-Purkinje cell synapse with neurexin and the glutamate-δ2 (Gluδ2) receptor and promotes synaptic stability (Cheng et al 2016). A decrease in Cbln1 levels could account for weakened connectivity and functionality between PFs and Purkinje cells (Kurihara et al 1997, Hirai et al 2005). As the link between UBE3A and ASD emerged, I measured the protein expression level of Ube3A in the cerebella of patDp/+, matDp/+, and WT mice. I hypothesized that patDp/+ mice would show increased Ube3A expression relative to WT and matDp/+ mice based on their autistic-like behavioral symptoms and altered glutamatergic synaptic transmission at CF- and PF-Purkinje cell synapses.

Advantages of Two Different Mouse Models of ASD: The 15q11-13 mouse model of ASD presents two distinct advantages from a research perspective: it is the most penetrant and frequent genetic aberration seen in ASD and the mouse model shows strong face validity (Cook & Scherer 2008). However, the 15q11-13 duplicated chromosomal region encompasses several

genes, making it difficult to associate specific genes with symptomatic-like behaviors. In order to circumvent the challenges presented by working with the 15q11-13 mouse model of ASD, I obtained CYFIP1 OE mice.

Oguro-Ando and colleagues identified CYFIP1 as an important candidate gene for association with ASD pathology when they revealed that CYFIP1 was overexpressed in post-mortem brain tissue (superior temporal gyrus) from 15q11-13 patients who had been diagnosed with ASD (Oguro-Ando et al 2015). CYFIP1 controls a complex network of proteins, which has been linked to ASD (Rogers et al 2001), as well as Fragile X syndrome (Schenck et al 2001). Endogenous CYFIP1 represses the initiation of translation at synapses by forming a complex with eIf4E (a translation initiation factor) and FMRP (Napoli et al 2008). Additionally, CYFIP1 has been implicated in the coordination of cytoskeletal remodeling as well as the formation and maintenance of dendritic spines by modulating the mTOR pathway (Tang et al 2014, Oguro-Ando et al 2015)

The CYFIP1 OE mouse model of ASD is less clinically relevant than the 15q11-13 mouse model because while CYFIP1 expression in patients was increased, the specific laboratory-induced genetic aberration causing CYFIP1 to be overexpressed in the mouse model has not been naturally observed in patients. However, the benefits of working with this new mouse model may outweigh the drawbacks. Notably, the CYFIP1 OE mouse model of ASD overexpresses just one gene: CYFIP1 (Geschwind Lab, unpublished). Modulations of behavior or synaptic activity can be associated with the altered levels of CYFIP1 and its targets. Additionally, CYFIP1 is a non-imprinting gene, which eliminates the hazy situation surrounding human imprinting and how it carries over to mice. Several studies have explored a role for CYFIP1 (Pathania et al 2014, Gkogkas et al 2013, Waltes et al 2014) in connection with autism-

like symptoms, but few have yet to explore the effect of overexpressing CYFIP1 on synaptic transmission in the cerebellum. In order to test whether CYFIP1 OE mice showed similar synaptic impairments to patDp/+ mice, CF-Purkinje cell synaptic transmission was measured in the new mice.

Materials and Methods

All procedures are in accordance with the guidelines set by the Institutional Animal Care and Use Committee of the University of Chicago.

Slice preparation: Cerebellar vermis from CYFIP1 OE mice and their WT littermates was dissected and separated into sagittal slices (200 μm) after isoflurane anesthesia. Slices were prepared using a vibratome (Leica VT1200S) with a ceramic blade. Slices were cut in 4 ºC standard ACSF (as described in Chapter 2 Methods), and bubbled with 95% O_2 and 5% CO_2 (pH 7.4). After slicing, sections were transferred to a storage chamber where they incubated for 90 minutes at RT in ACSF.

Somatic whole-cell patch clamp recordings: Recordings were done under 40x or 63x magnification using an EPC 10 Amplifier (HEKA Electronics) and a Zeiss LSM 5 Exciter, Axioskop 2 microscope. Slices were continuously perfused in standard ACSF supplemented with 100 μM picrotoxin (Sigma). Purkinje cell somata were patch-clamped at RT at a holding potential of -70 mV with a glass micropipette (2.5-5.5 MΩ) containing the following in mM: 150 CsCl, 4.6 $MgCl_2$, 10 HEPES Acid, 1 EGTA, 0.1 $CaCl_2$, 4 ATP-Na, and 0.4 GTP-Na (pH 7.25-7.35). Stimulation electrodes were placed in the granular layer for CF-EPSC recordings. CFs

were stimulated twice, separated by 100 ms, every 20 s. Series and input resistances were monitored by inducing hyperpolarizing voltage steps (-10 mV) for 100 ms at the end of each sweep.

Western blot: For Western blot analysis of activity-regulated cytoskeleton-associated protein (Arc) and of UBE3A, murine cerebellar tissue from 15q11-13 mice (WT, patDp/+, and matDp/+) was collected after anesthesia by isoflurane and snap-frozen on dry ice. Whole protein extracts were then obtained by Teflon pestle homogenization in tissue lysis buffer (50 mM tris(hydroxymethyl)aminomethane (TRIS) pH 7.5, 150 mM NaCl, 0.5% Na-Deoxicholate, 1% Nonidet P-40, 10% Glycerol, 2% EDTA, 1% Sigma-Aldrich protease inhibitor cocktail). The homogenate was centrifuged for 15 min at 16000xg at 4 ºC, and the supernatant was collected, aliquoted, and frozen at -80 ºC. Protein extracts were quantified to determine protein concentration (Pierce BCA protein assay kit). 25 µg of protein extract was loaded into each well of a 10% SDS-polyacrylamide precast gel (Biorad). Gels were blotted on PVDF membranes, and immunodetection was carried out using anti-UBE3A (mouse, 1:200, 2 nights, BD Transduction Laboratories), anti-Arc (mouse, 1:1,000, overnight, Synaptic Systems), and anti-β-actin (mouse, 1:10,000, 45 min, Sigma) as primary antibodies. Horseradish peroxidase (HRP) conjugated secondary antibody (goat anti-mouse, 1:30,000, 1 hr, Millipore) was used. ECL-Plus (Amersham) was used to visualize signals. Images were exported and subjected to densitometric quantification of bands using ImageJ (NIH). Values were normalized to β-actin levels and were reported relative to WT average expression levels.

Data analysis: Electrophysiological data analysis was performed using Excel (Microsoft) and Patchmaster (HEKA Electronics). Electrophysiological data were quantified using the Mann Whitney Test. Western blot data were analyzed using ImageJ (NIH) for densitometric quantification and a one-way ANOVA with post-hoc Tukey Tests to test for significance.

Results

After examining alterations in the synaptic activity of excitatory inputs to Purkinje cells, I explored specific genes within the 15q11-13 chromosomal region to determine which of those genes might be involved in the observed synaptopathies. I examined protein levels of Ube3a by Western blot in both the cerebellar vermis and hemispheres (Figure 9a). P10-12 patDp/+ mice show increased levels of Ube3a (Figure 9b, Vermis: WT 100% ± 5.80, n=14; patDp/+ 119.368% ± 6.596, n=7; matDp/+ 143.776% ± 5.989, n=8. Hemispheres: WT 100% ± 6.190, n=16; patDp/+ 125.904% ± 3.016, n=8; matDp/+ 161.363% ± 4.073, n=8.). Surprisingly, matDp/+ mice show levels of Ube3a protein that are even higher than that of patDp/+ mice in both the vermis and hemispheres.

Arc is a protein found at synapses that is involved with the mechanisms of PF-LTD (Guzowski et al 2000, Plath et al 2006, Okuno et al 2012, Wang et al 2016). Additionally, Arc is a downstream target of Ube3a. Despite changes in Ube3a levels among the genotypes, there was no change in P10-12 Arc protein expression (Figure 9a, 9b, Vermis: WT 100% ± 4.75, n=16; patDp/+ 93.117% ± 5.068, n=8; matDp/+ 93.117% ± 5.068, n=8, one-way ANOVA P=0.537. Hemispheres: WT 100% ± 7.210, n=16; patDp/+ 120.231% ± 9.049, n=8; matDp/+ 96.342% ±6.046, n=8, one-way ANOVA p=0.067).

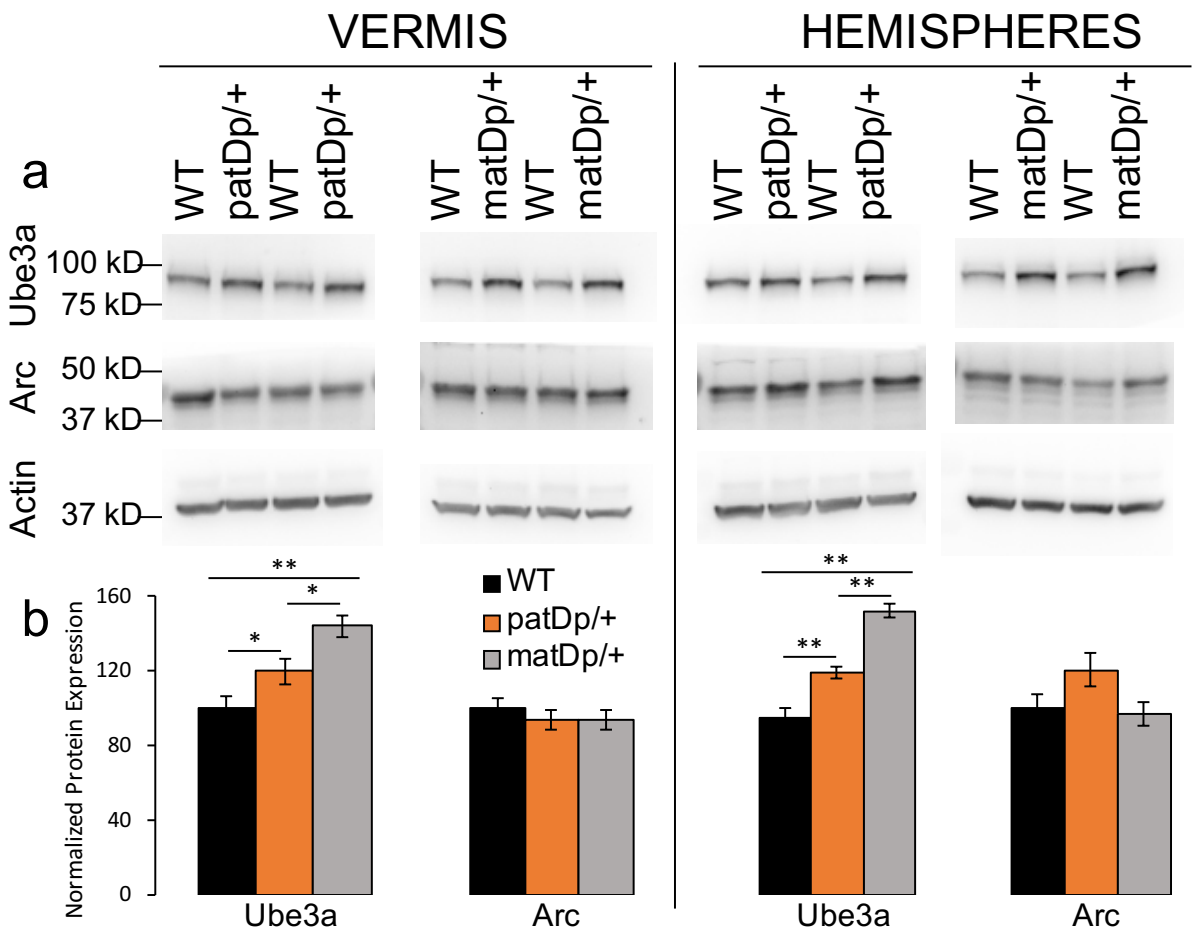

Figure 9: Cerebellar Ube3A protein expression is enhanced in patDp/+ and matDp/+ mice compared to WT littermates. a) Western blot images for Ube3a (top), Arc (middle), and Actin (bottom) in the cerebellar vermis (left) and hemispheres (right). b) Quantification of Ube3a and Arc expression levels normalized to Actin and expressed as a percentage of WT levels. Whole protein extracts from the cerebellar vermis and cerebellar hemispheres were blotted and quantified separately. Results were comparable in both regions. *p<0.05, **p<0.01, one-way ANOVA and post-hoc Tukey tests.

To explore correlations between the genes in the 15q11-13 conserved linkage group and the physiology we observed in patDp/+ autistic-like mice, we obtained mice that overexpress CYFIP1. After testing synaptic transmission at CF-Purkinje cell synapses, I determined that CYFIP1 OE mice show mildly enhanced CF-EPSCs compared to WT mice in both the CYFIP1 and 15q11-13 colonies (Figure 10a, CYFIP1 OE: 1.89 nA ± 0.11, Combined WT 1.37 nA ± 0.11, Mann Whitney Test p = 0.0151), but the amplitudes are not as large as CF-EPSCs recorded from

patDp/+ mice (patDp/+ and 15q11-13 WT data shown in Figure 4b, Mann Whitney Test p = 0.0198) at holding potentials of -30 mV (Figure 10a, b), but not -70 mV (Figure 10c, d). CF-EPSCs were recorded at more depolarized potentials in order to have better control over the voltage clamp while passing such large currents. (The sample size of recordings from CYFIP1 OE mice at -70 mV is insufficient to calculate meaningful statistics for significance. Additional recordings are needed.) CF-EPSCs from WT mice from the two colonies were combined because their amplitudes are not significantly different from each other. The middle range amplitude displayed by CF-ESPCs recorded at -30 mV from CYFIP1 OE mice suggests that the overexpression of CYFIP1 does indeed contribute to the synaptopathological phenotype in the cerebellar circuitry during development, but that it is not responsible for the full enhancement of CF-EPSCs. It is likely that CYFIP1, as well as other proteins in the conserved linkage group, may play an additional role in affecting development at CF-Purkinje cell synapses.

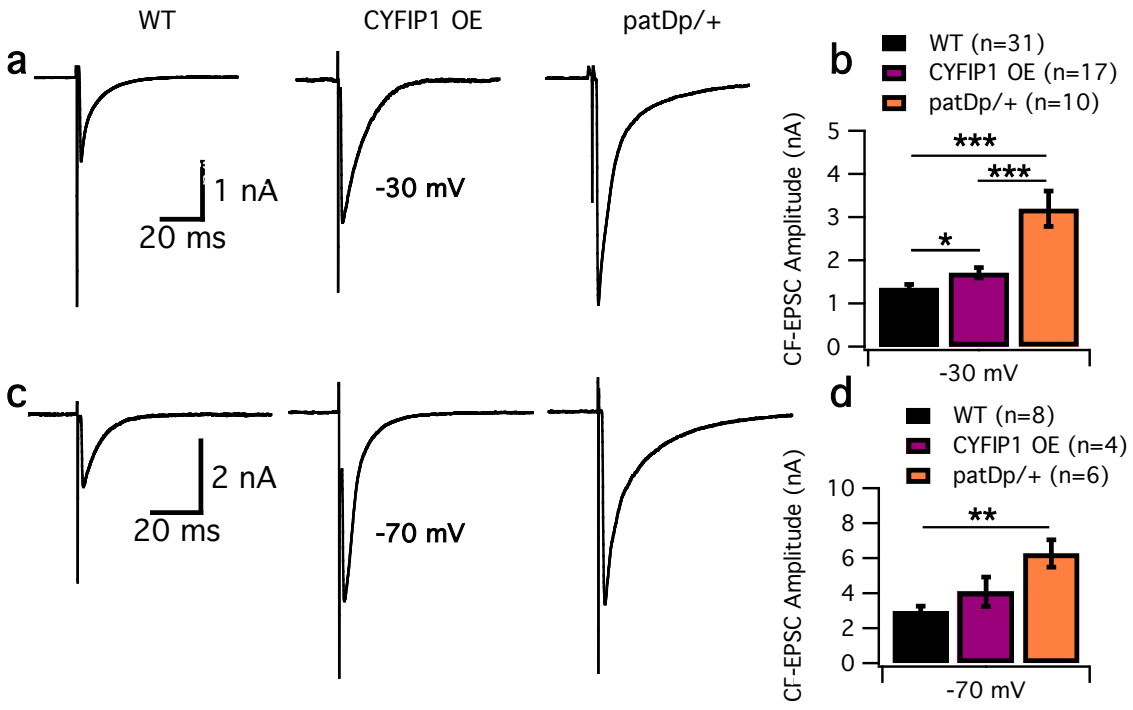

Figure 10: CF-EPSCs are mildly enhanced in CYFIP1 OE mice.

Figure 10, continued. CF-EPSCs are mildly enhanced in CYFIP1 OE mice.
a) Representative traces of CF-EPSCs at a holding potential of -30 mV in WT (left), CYFIP1 OE (middle), and patDp/+ (right) mice. WT CF-EPSC recordings from the 15q11-13 colony and the CYFIP1 colony were not significantly different from each other, so they were combined. b) Quantification of all CF-EPSCs recorded at -30 mV in the three genotypes. c) Typical traces of CF-EPSCs at a holding membrane voltage of -70 mV in WT (left), CYFIP1 OE (middle), and patDp/+ (right) mice. Again, WT CF-EPSC recordings from the 15q11-13 colony and the CYFIP1 colony were not significantly different from each other, so they were combined. d) Average of all CF-EPSCs recorded at -70 mV in the three genotypes. Mann Whitney Test, *$p<0.05$, **$p<0.01$, ***$p<0.001$.

Discussion

One challenge of working with the 15q11-13 mouse model of ASD is that the duplicated chromosomal region encompasses approximately twenty genes (depending on the breakpoints). This genetic aberration is highly clinically relevant because the same copy number variation mutation has been observed in patients (Cook & Scherer 2008, Urraca et al 2013); however, the length of the region makes it difficult to identify which genes are associated with ASD symptoms. In an effort to select a candidate gene and associate it with ASD symptoms, I first focused on Ube3a because its deletion is already causally linked to Angelman syndrome and Prader-Willi syndrome (Albrecht et al 1997, Dindot et al 2008, Heck et al 2008). As a gene whose expression level is relevant for these social-affective syndromes, I predicted that overexpression instead of underexpression/deletion might also be relevant to a related disorder: ASD. I predicted that the level of Ube3a was tightly regulated, and that altered levels of the Ube3a protein could be associated with a disorder phenotype. However, the result obtained from Western blots on cerebellar whole cell extracts presented an unclear result: patDp/+ mice showed higher Ube3a expression than WT mice, and matDp/+ mice showed even higher Ube3a expression - higher than levels observed in both WT and patDp/+ mice. The reason this result is unclear is that matDp/+ mice display a behavioral and physiological phenotype very similar to a

WT phenotype, in that they do not show autistic-like symptoms or synaptic pathology. This perplexing result seems to indicate that a low or very high level of Ube3a expression may be protective against autistic-like symptoms, but that a middle range of Ube3a protein expression can be associated with ASD. Another possibility, given the imprinting pattern and the size of the duplication, is that overexpressed genes interact with each other in complex ways. In this scenario, it is plausible that the overexpression of a different gene is protecting against the elevated levels of Ube3a.

An additional limitation of conducting western blots for Ube3a and Arc proteins in Purkinje cells is that whole tissue extracts from the cerebellum were used. More specifically, Ube3a and Arc are expressed in Purkinje cells at synapses, but the tissue tested contained Purkinje cells, basket cells, stellate cells, CFs, and many granule cells. Ube3a expression has been observed in molecular layer interneurons as well as Golgi cells in the granular layer, though both cell types show expression levels that are less robust than seen in Purkinje cells (Bruinsma et al 2015). Since Ube3a is expressed in multiple cell types in the cerebellar cortex, the signal cannot be interpreted as an isolated signal from Ube3a in Purkinje cells. In the future, experiments may be improved by measuring levels of Ube3a or Arc using single-cell real-time polymerase chain reaction (RT-PCR.)

CYFIP1 is a protein whose overexpression has been repeatedly noted for its association with symptoms of ASD (Rogers et al 2001, Oguro-Ando et al 2015). CYFIP1 falls on the edge of the 15q11-13 conserved linkage group, and is duplicated along with the copy number variation mutation in about 30% of 15q11-13 patients. Aside from the rest of the conserved linkage group, increases in CYFIP1 are known to repress the initiation of translation in synapses by working in a complex with eIF4E and FMRP (Napoli et al 2008, Tang et al 2014). In order to

study the effects of overexpressing CYFIP1 in isolation, CYFIP1 OE mice were used instead of 15q11-13 patDp/+ mice.

Measurements of CF-EPSCs in CYFIP1 OE mice show mild but significant enhancement over CF-EPSCs recorded from WT mice, but were also significantly smaller than CF-EPSCs from patDp/+ mice (Figure 10b). The mild enhancement of CYFIP1 OE CF-EPSC amplitudes reflects that overexpression of CYFIP1 may increase synaptic transmission between CFs and Purkinje cells, but that it cannot be responsible for the entire enhancement displayed in patDp/+ mice. It is likely that CYFIP1 is just one of the genes in the 15q11-13 region that contribute to enhancing CF-Purkinje cell synaptic transmission. The overexpression of several of these genes together may be responsible for the full increase of CF-EPSC strength. Based on the results of this experiment, I would predict that VGluT2 staining in CYFIP1 OE mice would show increased density of CF-Purkinje cell synapses, but less of an increase than was observed in patDp/+ mice. It is possible that PF-Purkinje cell signaling may also be affected, possibly to a mild extent. If such an impairment is found in both excitatory inputs to synaptic transmission to Purkinje cells in CYFIP1 OE mice, then it would be important to look for possibly alterations to synaptic plasticity. In the future, it will be tedious but important to systematically go through each gene in the 15q11-13 copy number variation to determine its potential effect on ASD-like synaptic pathology. Since the 15q11-13 chromosomal region encompasses several genes who likely interact in complex ways that have yet to be explored, it will additionally be necessary to examine combinatory effects.

Chapter 5: General Discussion

ASD is marked by hallmark symptoms including social deficits, difficulties with communication, and increased repetitive behaviors. Many studies focus only on these core features, often overlooking motor pathology that is present in approximately 80% of patients (Green et al 2009, Fournier et al 2010). The motor pathology involves difficulties controlling eye movements, clumsy gait, and impaired eyeblink conditioning, suggesting that the cerebellum is highly involved in ASD (Johnson et al 2013, Mosconi et al 2013). In fact, the cerebellum is one of the most consistently affected brain regions in ASD (Fatemi et al 2012, Wang et al 2014). In order to learn about how the cerebellar circuitry underlying eyeblink conditioning is impaired in ASD, Piochon et al 2014 used the 15q11-13 mouse model of ASD and determined that LTD is disrupted at the PF-Purkinje cell synapse in patDp/+ mice. This dissertation research carries forward the findings in Piochon et al 2014 to examine which part of the cerebellar circuit may be responsible for the failure of LTD induction at PF-Purkinje cell synapses. In addition to exploring synaptic transmission and calcium signaling at PF-Purkinje cell and CF-Purkinje cell synapses, I explored UBE3A and CYFIP1 as candidate genes for ASD synaptic pathology.

Examining cerebellar development in mouse models of ASD presents strong advantages. Notably, the cerebellum is relatively conserved over vertebrate evolution relative to other brain regions (Bell 2002). Cerebellar studies in mice transfer more easily to patients than studies conducted on other, more recently evolved brain regions. Furthermore, intact cerebellar function is critical for proper eyeblink conditioning (McCormick and Thompson 1984). Numerous studies have revealed that eyeblink conditioning is affected in mouse models of ASD as well as patients (Sears et al 1994, Oristaglio et al 2013). Unlike eyeblink conditioning, most behaviors – in both humans and mice – cannot be clearly associated with specific brain regions. Eyeblink

conditioning however, is the exact same, testable behavior in patients and mice. With further exploration and expansion of eyeblink conditioning tests in patient populations, information about correlating specific genetic aberrations with ASD phenotypes may be possible. Additionally, it may become important to employ eyeblink conditioning as a biomarker of ASD (Reeb-Sutherland, Fox 2015) since it is a clearly understood behavior with well-studied underlying circuitry that develops before the classic hallmark symptoms begin to appear. In such a paradigm, earlier diagnosis in patients could lead to earlier behavioral and potential therapeutic interventions.

Despite the numerous advantages of research on the murine cerebellum in models of ASD, it is imperative to remember that mice are not humans. Although mice can display autistic-like behaviors, they will never show the exact same ASD phenotype and symptoms that patients display. For obvious reasons, however, it would have been unethical to conduct the experiments discussed in this dissertation on patients. While it would be ideal to simplify the model even more – to studying a simple computer model of the brain, such a model does not exist. To date, we do not have sufficient knowledge about the brain to create a meaningful model for this type of research. In order to learn new knowledge about the brain, research must be performed on actual brains.

Disruptions of Synaptic Transmission and Connectivity at Glutamatergic Inputs to Purkinje Cells

Chapter in Review: In chapter 2, it was revealed that there is a disruption to cerebellar excitatory synaptic transmission and to calcium buildup in patDp/+ mice. CF input to Purkinje cells is dramatically enhanced, as seen by measuring CF-evoked EPSCs. Additional investigation into

connections made between CFs and Purkinje cells shows that the density of VGluT2, a marker for CF-Purkinje cell synapses, is increased on large caliber dendrites where CFs typically contact Purkinje cells. Notably, ectopic VGluT2 synapses were also observed on Purkinje cell fine dendrites, territory which is generally considered to be reserved for PF synapses. After examining changes between CFs and Purkinje cells, evidence of an imbalance between excitatory inputs to Purkinje cells emerged. Specifically, it was noted that patDp/+ mice, in addition to having enhanced CFs, have weak PFs. Weaknesses in PF-Purkinje cell synaptic transmission were measured with trains of 5 PF-evoked EPSPs. In patDp/+ mice, Purkinje cell responses to PF-EPSPs show lower amplitudes than in WT littermates and matDp/+ mice. To address the question of whether calcium buildup during spike timing-dependent plasticity is also impaired, the ratio of the amplitudes of two PF stimulations at different interstimulus intervals was measured. Indeed, it appears that at short interstimulus intervals, paired pulse facilitation is reduced in patDp/+ mice.

Significance and Future Directions: Enhanced CF synaptic transmission, and specifically the overabundance and ectopic nature of CF-Purkinje cell synapses, is very likely an underlying circuit issue that can be associated with faulty synaptic plasticity in patDp/+ mice. When the process of CF-elimination is delayed in patDp/+ mice, numerous issues may arise, including but not limited to the elongated presence of multiple CFs, CFs making synapses on the wrong part of Purkinje cell dendrites, and CF synapses either taking over or filling in empty space where PFs should be able to make synapses. Weak PF signaling to Purkinje cells – whether it develops before or after the aberrant CF development – is also a critical circuit issue that can likely explain the deficits in PF-LTD in patDp/+ mice. To further explore the issue of cerebellar

glutamatergic circuitry underlying synaptic plasticity deficits, it would be useful to look for similar circuit impairments in other mouse models of ASD. patDp/+ mice are not the only autistic-like mice to show impaired PF-LTD. Changes in or impairments to synaptic plasticity have also been identified in Neuroligin3-KO (Baudouin et al 2012) and Shank3+/ΔC (Peça et al 2011) mouse models of ASD. A comparison between mouse models of ASD could inform how particular enhanced or weakened parts of the PF-LTD induction protocol contribute to its success or lack thereof. Though PF-LTD is altered in several mouse models of ASD, it is sometimes seen as enhanced, sometimes reversed as potentiation, and sometimes impossible to induce without additional manipulations (Peça et al 2011, Baudouin et al 2012, Piochon et al 2014, Simmons et al 2018 *in preparation*). Changes to the underlying circuitry are likely different in each of these three cases, and further experimentation on this can provide insight about how particular insults to circuit development affect the success of synaptic plasticity. Importantly, we can associate better understanding of how and why cerebellar synaptic plasticity may fail, with effects on eyeblink conditioning in both mice and human patients.

Defects in the development of cerebellar circuitry, including neonatal cerebellar injury as well as changes to synaptic transmission and plasticity, affect the development of other brain regions, especially cortical structures (Wang et al 2014). The cerebellum connects through long-range loops to several cortical structures through the thalamus. Evidence shows that insults to cerebellar circuitry during critical periods of growth and circuit refinement affect the development of cortical brain regions (Wang et al 2014). These affected cortical regions are largely responsible for the classical symptoms observed in ASD, such as impaired sociality, increased perseverative behavior, and difficulties with communication. Testing for the ability to associate multisensory stimuli on a millisecond timescale using eyeblink conditioning can reveal

whether the underlying cerebellar circuitry is intact. Additionally, abnormalities in eyeblink conditioning indicate that it may be worthwhile to examine whether the circuit defect appeared before the deficient cortical structures.

In addition to deciphering how circuit modulations may affect synaptic plasticity and eyeblink conditioning, it is important to zoom in on the circuit defects to look at underlying genetic aberrations. In order to more fully explore weakened PF signaling to Purkinje cells, an exploration into levels of neurexin1 and Cbln1 may provide much needed insight into the stability of PF-Purkinje cell synapses. Neurexin1 is a presynaptic scaffolding protein that is expressed in presynaptic PF terminals, and it forms a complex with Cbln1 that binds to the Gluδ2 receptor in postsynaptic Purkinje cell terminals (Cheng et al 2016). Together, these three proteins stabilize PF-Purkinje cell synapses (Cheng et al 2016, review: Reissner et al 2013). PF signaling to Purkinje cells may very well be weakened by lower or mutated expression of any of these three proteins, or could be experimentally modulated and enhanced by higher protein expression. Importantly though, it will be necessary to keep in mind that overexpression of Cbln1 may provide a "double negative" phenotype and prevent full PF-Purkinje cell synapses from forming if it binds neurexin1 and Gluδ2 receptors independently of each other instead of together in one complex.

Beyond exploring connections with molecular mechanisms and eyeblink conditioning, a study which has yet to be conducted is an exploration into possible changes in spike thresholds in patDp/+ mice compared with WT mice. It was observed that PF-EPSPs recorded from patDp/+ mice show a much lower probability of spiking than PF-EPSPs recorded from WT mice. However, this result may be affected by the lower amplitude EPSP generated from the same stimulus intensity. In order to test spiking probability in a more consistent manner, the size of

the EPSP would have to be set to a constant amplitude. Alternatively, stimulation by somatic depolarization would circumvent the difficulty of keeping EPSP amplitudes consistent across cells, mice, and genotypes.

Deficient Calcium Signaling at PF-Purkinje Cell Synapses Impairs Plasticity, but is Rescued Pharmacologically

Chapter in Review: In chapter 3, reductions in calcium signaling that accompany weak PF synaptic transmission to Purkinje cells were unveiled. Abnormally low amplitude calcium transients were observed during the two protocols that involved PF synaptic transmission: PF-LTP (100 Hz PFb) and PF-LTD (100 Hz PFb+CF). Calcium transients in Purkinje cell spines that were measured in response to CF-evoked stimulation alone were unaltered. Because low levels of calcium signaling were observed in Purkinje cell spines during the PF-LTD induction protocol in patDp/+ mice, postsynaptic calcium influx was pharmacologically enhanced in an effort to rescue PF-LTD. With this manipulation, PF-LTD was successfully restored to WT levels in patDp/+ mice.

Significance and Future Directions: The fact that PF-LTD was rescued in patDp/+ mice with the addition of pharmacological intervention to increase postsynaptic calcium influx strongly suggests that deficient calcium signaling was responsible for the previously impaired PF-LTD. Spine calcium imaging data confirm that calcium transients evoked by PF stimulation are indeed weaker in Purkinje cell spines from patDp/+ mice as compared with WT littermates and matDp/+ mice.

The cerebellar circuit in patDp/+ mice has been shown to exhibit delays in CF developmental pruning and deregulation of PF-LTD (Piochon et al 2014). Importantly, synaptic plasticity and synaptic pruning at PF-Purkinje cell synapses share similar molecular machinery (Piochon et al 2016, Hansel 2018). The overlap of these two processes suggests that developmental defects in the circuit can predict lasting deficits in the regulation of synaptic plasticity. Altered levels of translation due to changes in expression of the CYFIP1 pathway may cause synaptic abnormalities that are associated with ASD. In turn, the CYFIP1 pathway may be involved in LTD deregulation in adulthood, which can be correlated with previously altered synaptic pruning during development (review: Hansel 2018).

If circuit development issues cannot be remedied for ASD patients or autistic-like mice, strategies that therapeutically increase calcium entry to Purkinje cells may be useful down the line. While interventional changes to circuit development would perhaps have to be performed very early in life – possibly before the traditional ASD symptoms are even present – therapeutic strategies designed to increase calcium influx could potentially be put into place at later time points. Compounds such as ampakines, which effectively increase postsynaptic calcium influx by promoting prolonged depolarization, are not currently used therapeutically, but there may be potential in this field that has yet to be explored. A therapeutic strategy that increases calcium influx would need to be carefully titrated. A serious potential pitfall of this type of therapeutic strategy is that extreme increases in intracellular calcium concentration are associated with apoptosis.

If such a strategy could be put into place, and if it could rescue motor learning deficits in eyeblink conditioning, then a similar strategy could be investigated for other brain regions with synaptic plasticity impairments in autistic-like mice. To be clear though, links between circuitry,

plasticity, and behavior have not been clearly defined in areas of the brain that are responsible for more cognitive behaviors involving social interaction, perseverative behaviors, and communication. Extensive additional research would need to be applied to make these links between circuit function and cognitive behaviors. To begin, it will be important to consider that cortical dysfunction can be downstream from cerebellar dysfunction (Wang et al 2014). Often, neonatal injury or insult to the cerebellar circuitry has a high likelihood of manifesting as ASD (Wang et al 2014).

Before increasing postsynaptic calcium influx, it may be useful to determine the root cause of the weak calcium signaling at PF – Purkinje cell synapses. Do the PFs fail to accumulate as much calcium in presynaptic terminals of patDp/+ mice compared with WT mice? How does this affect vesicle release? Is the subunit composition of the AMPA receptors in Purkinje cells different in patDp/+ mice than in WT mice? Answers to these questions would provide additional targets for therapeutic strategies, and would also lead to insights about the mechanisms behind ASD motor pathology.

Candidate Genes for Association with ASD Symptoms in the 15q11-13 and CYFIP1 OE Mouse Models of ASD

Chapter in Review: In chapter 4, an effort to pin down genes underlying the autism-like symptoms seen in mice manifested as an examination of Ube3a, Arc, and CYFIP1 as candidate genes. Western blot results from whole protein extracts of cerebellar tissue in 15q11-13 mice show upregulation of Ube3a protein in patDp/+ mice compared to WT mice, and even higher expression in matDp/+ mice. In contrast, levels of Arc, a downstream target of Ube3a, are unaffected by genotype. One complication of working with the 15q11-13 mouse model of ASD

is that expression levels of many different proteins arising from the duplicated region are affected. As such, it is challenging to determine which of the potentially affected proteins can be associated with autism-like symptoms. To address this, I obtained and began to study the glutamatergic cerebellar circuitry in a mouse model of ASD that specifically overexpresses CYFIP1 without intentionally manipulating any other genes (excluding downstream targets of CYFIP1). CF-Purkinje cell synaptic transmission in CYFIP1 OE mice is mildly but significantly increased compared to WT mice, but is not as strong as the increase in CF-EPSC amplitude observed in patDp/+ mice.

Significance and Future Directions: As previously discussed, the 15q11-13 mouse model of ASD was selected for these experiments because it represents one of the most frequent and penetrant genetic abnormalities seen in patients. Genetic aberrations account for about 20% of all ASD cases in patients, and duplications of the 15q11-13 conserved linkage group account for 1-3% of all ASD cases (Cook & Scherer 2008). By calculation, we can deduce that the 15q11-13 mutation accounts for 5%-15% of the cases of ASD that are caused by genetic aberrations. While this provides an advantage in studying an aberration that affects many patients, it also presents challenges since the duplicated region encompasses approximately 20 genes. Without a systematic evaluation of each gene, as well as combinations of genes, in this region, it is difficult to know which of the genes can be associated most strongly, or at all, with symptoms.

In effort to circumvent this challenge, Ube3a was chosen for investigation because it is already known to be causally associated with Angelman syndrome and Prader-Willi syndrome when deleted maternally and paternally, respectively (Albrecht et al 1997, Dindot et al 2008, Heck et al 2008). When levels of gene or subsequent protein expression are carefully regulated,

it is likely that an increase – or duplication – of expression, as well as a deletion may lead to pathology. After finding that Ube3a was indeed overexpressed in cerebellar tissue from patDp/+ mice, associations of Ube3a with pathology seemed promising. However, after finding that levels of Ube3a expression are even higher in cerebellar tissue from matDp/+ than patDp/+ mice, the result became more challenging to interpret. The result suggests a possible, albeit unusual, situation: WT and very elevated levels of Ube3a protect against ASD, while a moderately elevated level of Ube3a leads to ASD. Alternatively, it is more likely that Ube3a interacts with other proteins in the region in a complex way that we do not yet understand.

To further explore how increases in Ube3a expression may be involved with ASD pathology, future experiments should either include Western blots performed specifically on Purkinje cells instead of whole cerebellar extracts, or should focus on single cell RT-PCR in Purkinje cells. The reason to narrow the search exclusively to Purkinje cells is that in the cerebellum, Ube3a and Arc are highly expressed at Purkinje cell spines (Dindot et al 2008). In the cerebellum, Ube3a is most robustly expressed in Purkinje cells, but is also expressed to a lesser extent in Golgi cells and molecular layer interneurons (Bruinsma et al 2015). Alternatively, using immunohistochemistry to visualize Ube3a or Arc may provide useful insights about the location and quantity of these two proteins in patDp/+ mice compared with WT littermates.

Research by Oguro-Ando and colleagues revealed increased CYFIP1 levels in post-mortem brain tissue from ASD patients and in autistic-like mice (Oguro-Ando et al 2015). To follow up on CYFIP1 as a potential candidate gene for association with ASD symptoms, we obtained CYFIP1 OE mice in order to study the gene in isolation, and most importantly, away from manipulations affecting the rest of the genes in the 15q11-13 region. CYFIP1 falls between

breakpoint1 and breakpoint 2 on the proximal end of the region and stays attached to the duplicated segment much of the time (Chung et al 2016).

Preliminary investigation into circuit defects in the cerebellum revealed mild increases in CF-Purkinje cell synaptic transmission in CYFIP1 OE mice. To get a better understanding of the autistic-like phenotype in these new mice (Geschwind Lab, unpublished), additional experiments into PF-Purkinje cell synaptic transmission, synaptic plasticity, and calcium buildup can be conducted. If more impairments in glutamatergic synaptic transmission and buildup are found, it may be important to examine eyeblink conditioning to learn how they are affected or associated with the overexpression of CYFIP1. If such findings arise, one hypothetically productive, albeit labor-intensive, way to begin to look at combinations of candidate genes would be to use viral-mediated overexpression or knock-down of one or two additional genes at a time from the 15q11-13 region in the CYFIP1 OE and WT littermate mice. A different option would be to pharmacologically disrupt the downstream targets of CYFIP1. The inhibitor α-[2-[4-(3,4-Dichlorophenyl)-2-thiazolyl]hydrazinylidene]-2-nitro-benzenepropanoic acid (4EGI-1) is a specific molecule which disrupts the interaction between eIF4E and eIF4G (Moerke et al 2007, Gkogkas et al 2013, Santini et al 2013), which are both downstream of CYFIP1. In effect, such a pharmacological agent would appear physiologically as a decreased level of CYFIP1. This would ideally restore the activity of eIF4E and eIF4G in complex to WT levels, and perhaps rescue issues with potentially abnormal synaptic transmission, synaptic plasticity, spine calcium signaling, and eyeblink conditioning. Another way to examine which genes may be involved in combination with each other in the ASD phenotype would be to conduct a genome-wide associated study on ASD patients and then examine specific candidate genes in mouse models.

For now, studies linking cerebellar circuitry with synaptic plasticity and behavior in mice will continue to provide much needed insight about the underpinnings of synaptic and behavioral pathology that describes the aberrant development seen in ASD.

Associating Genetic Aberrations with Specific Symptoms

It has been estimated that 83% of ASD individuals have an inherited genetic aberration leading to the disorder (Sandin et al 2017). While many research groups have explored environmental effects on the presentation of ASD symptoms, the consensus remains that genetic mutations are the main cause of ASD (Sandin et al 2017). Knowing this, it would be helpful to genotype willing ASD individuals and their families in order to find out which genes are most affected. ASD patients exhibit a wide range of symptoms, talents, and challenges, all of which are on a scale of varying severity. The advantages of building a database of genetic aberrations are numerous. First, specific mutations could be associated with particular symptoms. Second, specific mutations could be correlated with severity of particular symptoms. Third, such a database would enable researchers to look for groups of genes that are commonly found mutated or acting together to affect symptoms and severity. Fourth, by administering a lifestyle survey to patients participating in the genotyping study, researchers would be able to address issues related to environmental triggers and genetic penetrance. Fifth, by genotyping neurotypical siblings, researchers would be able to study the mechanisms of imprinting patterns that lead to ASD symptoms when a copy number variation mutation is inherited from a particular parent, as is seen with the 15q11-13 duplication.

Post-mortem brain samples provide compelling evidence in studies of protein expression or anatomy, but are not useful in correlating changes in expression with behavioral symptoms.

Any symptomatic evidence associated with these samples would be anecdotal, and less reliable than an observation from a controlled study. In contrast, participants in a genotyping study could be observed over time as they age, and each behavioral symptom could be evaluated and tested rigorously. Despite the extremely useful body of knowledge this type of research would provide, it should be noted that a pitfall of this approach is that families may not be inclined to participate unless they personally benefit from the study. This type of study would be unlikely to help ASD families or individuals in the short term, but would rather provide important long-term insights about ASD.

Non-motor Functions of the Cerebellum Itself vs. of Downstream Projections

It has been widely recognized that the cerebellum, which is responsible for learning and fine-tuning new movements, has non-motor functions that are cognitive and affective (review: Steinlin and Wingeler 2013). Cerebellar dysfunction or improper development often leads to ASD symptoms. Indeed, cerebellar insult during critical periods of development increases the chances of developing ASD by 36% (Wang et al 2014). However, whether abnormal cerebellar development leads to improper development of cognitive and affective brain areas (Strick et al 2009), and in turn leads to cognitive ASD symptoms, or whether the cerebellum develops abnormally and itself leads to cognitive ASD symptoms is unknown. Certainly, the cerebellum forms long-range loops to communicate with downstream regions, and thus influences activity and development in distant circuits (Wang et al 2014). However, the cerebellum is known to affect cognition on its own as well. In the future, it will be helpful to distinguish between these two ideas. This knowledge will help future studies to place weighted importance to cerebellar influence over other brain regions by projection compared with direct cerebellar influence when

examining overlapping functions. This information will be useful for studies on systems-level interactions between the cerebellum and downstream brain regions, research of direct cerebellar non-motor functions, and investigations of how the balance of these two pathways is disrupted or altered in disorders involving cerebellar abnormalities. It will additionally be interesting to examine how the symptoms of such cerebellar abnormalities manifest when the defect occurs during critical periods of development compared with during adulthood.

Bibliography

Albrecht U, Sutcliffe JS, Cattanach BM, Beechey CV, Armstrong D, Eichele G, Beaudet AL. (1997). Imprinted expression of the murine Angelman syndrome gene, *Ube3a*, in hippocampal and Purkinje neurons. *Nat. Genetics.* 17, 75-78.

Albus JS. (1971). A theory of cerebellar function. *Math. Biosci.* 10, 25-61.

Angoa-Pérez M, Kane MJ, Briggs DI, Francescutti DM, Kuhn DM. (2013). Marble burying and nestlet shredding as tests of repetitive, compulsive-like behaviors in mice. *J. Vis. Exp.* 82, 50978.

Arai AC & Kessler M. (2007). Pharmacology of ampakine modulators: from AMPA receptors to synapses and behavior. *Curr. Drug Targets*. 8, 583-602.

Armstrong DM, Schild RF. (1970). A quantitative study of the Purkinje cells in the cerebellum of the albino rat. *J. Comparative Neurol.* 139, 449-456.

Artola A, Bröcher S, Singer W. (1990). Different voltage-dependent thresholds for inducing long-term depression and long-term potentiation in slices of rat visual cortex. *Nature*. 347, 69-72.

Baudouin SJ, Gaudias J, Gerharz S, Hatstatt L, Zhou K, Punnakkal P, Tanaka KF, Spooren W, Hen R, De Zeeuw CI, Vogt K, Scheiffele P. (2012). Shared syndromic pathophysiology in syndromic and nonsyndromic rodent models of autism. *Science.* 338, 28-132.

Bear MF, Cooper LN, Ebner FF. (1982). A physiological basis for a theory of synapse modification. *Science*. 237, 42-48.

Bell C. (2002). Evolution of Cerebellum-Like Structures. *Brain, Behavior and Evolution* 59: 312-326.

Bienenstock EL, Cooper LN, Munro PW. (1982). Theory for the development of neuron selectivity: orientation specificity and binocular interaction in visual cortex. *J. Neurosci.* 2, 32-48.

Bruinsma CF, Schonewille M, Gao Z, Aronica E, Judson MC, Philpot BD, Hoebeek F, van Woerden GM, De Zeeum CI, Elgersma Y. (2015). Dissociation of locomotor and cerebellar deficits in a murine Angelman syndrome model. *J. Clin. Investigation.* 125, 10.1172/JCI83541.

Carillo J, Nishiyama N, Nishiyama H. (2013). Dendritic translocation establishes the winner in cerebellar climbing fiber synapse elimination. *J. Neurosci*. 33, 7641-7653.

Carper RA & Courchesne E. (2000). Inverse correlation between frontal lobe and cerebellum sizes in children with autism. *Brain*. 123, 836-844.

Cesa R, Strata P. (2009). Axonal competition in the synaptic wiring of the cerebellar cortex during development and in the mature cerebellum. Review. *Neuroscience*. 162, 624-632.

Chang PK, Prenosil GA, Verbich D, Gill R, McKinney RA. (2014). Prolonged ampakine exposure prunes dendritic spines and increases presynaptic release probability for enhanced long-term potentiation in the hippocampus. *Eur. J. Neurosci.* 40, 2766-2776.

Cheng S, Seven AB, Wang J, Skiniotis G, Özkan E. (2016). Conformational plasticity in the transsynaptic neurexin-cerebellin-glutamate receptor adhesion complex. *Structure*. 24, 2163-2173.

Chung L, Weng X, Zhu L, Towers A, Kim IH, Jiang Y. (2016). Parental origin impairment of synaptic functions and behaviors in cytoplasmic FMRP interacting protein 1 (Cyfip1) deficiency mice. *Brain Res.* 1629, 340-350.

Choo M, Miyazaki T, Yamazaki M, Kawamura M, Nakazawa T, Zhang J, Tanimura A, Uesaka N, Watanabe M, Sakimura K, Kano M. (2017). Retrograde BDNF to TrkB signaling promotes synapse elimination in the developing cerebellum. *Nat. Commun*. 8, 195.

Coesmans M, Weber JT, De Zeeuw CI, Hansel C. (2004). Bidirectional parallel fiber plasticity in the cerebellum under climbing fiber control. *Neuron*. 44, 691-700.

Cook EH & Scherer SW. (2008). Copy-number variations associated with neuropsychiatric conditions. *Nature*. 455, 919-923.

Courchesne E. (1997). Brainstem, cerebellar and limbic neuroanatomical abnormalities in autism. *Curr. Opin. Neurobiol.* 7, 269-278.

Crépel F, Delhaye-Bouchaud N, Guastavino JM, Sampaio I. (1980). Multiple innervation of cerebellar Purkinje cells by climbing fibres in staggerer mutant mouse. *Nature.* 283, 483–484.

Crépel F, Jaillard D. (1991). Pairing of pre- and postsynaptic activities in cerebellar Purkinje cells induces long-term changes in synaptic efficacy *in vitro. J. Physiol.* 432, 123-141.

Crépel F, Mariani J, and Delhaye-Bouchaud N. (1976) Evidence for a multiple innervation of Purkinje cells by climbing fibers in the immature rat cerebellum. *J. Neurobiol.* 7, 567-578.

De Zeeuw CI, Simpson JI, Hoogenraad CC, Galjart N, Koekkoek SK, Ruigrok TJ. (1998). Microcircuitry and function of the inferior olive. *Trends Neurosci.* 21, 391-400.

Deacon RM. (2006). Digging and marble burying in mice: simple methods for in vivo identification of biological impacts. *Nat. Protoc.* 1, 122-124.

Dere E, Huston JP, De Souza Silva MA. (2007). The pharmacology, neuroanatomy and neurogenetics of one-trial object recognition in rodents. *Neuroscience & Biobehavioral Reviews.* 31, 673-704.

Dindot SV, Antalffy BA, Bhattacharjee MB, Beaudet AL. (2008). The Angelman syndrome ubiquitin ligase localizes to the synapse and nucleus, and maternal deficiency results in abnormal dendritic spine morphology. *Human Mol. Genetics.* 17, 111-118.

Eccles JC, Llinás R, Sasaki K. (1966). The excitatory synaptic action of climbing fibres on the Purkinje cells of the cerebellum. *J. Physiol.* 182, 268-296.

Fatemi SH, Aldinger KA, Ashwood P, Bauman ML, Blaha CD, Blatt GJ, Chauhan A, Chauhan V, Dager SR, Dickinson PE, Estes AM, Persico AM, Sweeney JA, Webb SJ, Welsh JP. (2012). Consensus paper: pathological role of the cerebellum in autism. *Cerebellum*. 11, 777-807.

Fournier KA, Hass CJ, Naik SK, Lodha N, Cauraugh JH. (2010). Motor coordination in autism spectrum disorders: a synthesis and meta-analysis. *J. Autism Dev. Disord.* 40, 1227-1240.

Freeman JH, Steinmetz AB. (2011). Neural circuitry and plasticity mechanisms underlying delay eyeblink conditioning. *Learn Mem*. 18, 666-677.

Gkogkas CG, Khoutorsky A, Ran I, Rampakakis E, Nevarko T, Weatherill DB, Vasuta C, Yee S, Truitt M, Dallaire P, Major F, Lasko P, Ruggero D, Nader K, Lacaille JC, Sonenberg N. (2013). Autism-related deficits via dysregulated eIF4E-dependent translational control. *Nature. 493, 371.*

Goodlett CR & Mittleman G. Editor: Conn MP. (2017). Conn's Translational Neuroscience, Chapter 9 – The Cerebellum. Elsevier. Pp 191-212.

Green D, Charman T, Pickles A, Chandler S, Loucas T, Simonoff E, Baird G. Impairment in movement skills of children with autistic spectrum disorders. (2009). *Dev. Med. Child Neurol.* 51, 311-316.

Greer PL, Hanayama R, Bloodgood BL, Mardinly AR, Lipton DM, Flavell SW, Kim T, Griffith EC, Waldon Z, Maehr R, Ploegh HL, Chowdhury S, Worley PF, Steen J, Greenberg ME. (2010). The Angelman syndrome protein Ube3a regulates synapse development by ubiquitinating arc. *Cell*. 140, 704-716.

Guzowski JF, Lyford GL, Stevenson GD, Houston FP, McFaugh JL, Worley PF, Barnes CA. (2000). Inhibition of activity-dependent arc protein expression in the rat hippocampus impairs the maintenance of long-term potentiation and the consolidation of long-term memory. *J. Neurosci.* 20, 3993-4001.

Hansel C. (2018). Deregulation of synaptic plasticity in autism. *Neuroscience Letters.* https://doi.org/10.1016/j.neulet.2018.02.003.

Hansel C, Artola A, Singer W. (1997). Relation between dendritic Ca^{2+} levels and the polarity of synaptic long-term modifications in rat visual cortex neurons. *Eur. J. Neurosci.* 9, 2309-2322.

Hashimoto K & Kano M. (2013). Synapse elimination in the developing cerebellum. *Cell. Mol. Life. Sci*. 70, 4667-4680.

Hashimoto K, Miyazaki TM, Kitamura K, Yamazaki M, Shin HS, Watanabe M, Sakimura K, Kano M. (2011). Postsynaptic P/Q-type Ca^{2+} channel in Purkinje cell mediates synaptic competition and elimination in developing cerebellum. *Proc. Nat. Acad. Sci*. 108, 9987-9992.

Heck DH, Zhao Y, Roy S, LeDoux MS, Reiter LT. (2008). Analysis of cerebellar function in Ube3a-deficient mice reveals novel genotype-specific behaviors. *Hum. Mol. Genet.* 17, 2181-2189.

Hirai H, Pang Z, Bao D, Miyazaki T, Li L, Miura E, Parris J, Rong Y, Watanabe M, Yuzaki M, Morgan JI. (2005). Cbln1 is essential for synaptic integrity and plasticity in the cerebellum. *Nat. Neurosci.* 8, 1534-1541.

Hirano T. (1990). Depression and potentiation of the synaptic transmission between a granule cell and a Purkinje cell in rat cerebellar culture. *Neurosci. Lett.* 119, 141-144.

Ichikawa R, Miyazaki T, Kano M, Hashikawa T, Tatsumi H, Sakimura K, Mishina M, Inoue Y, Watanabe M. (2002). Distal extension of climbing fiber territory and multiple innervation caused by aberrant wiring to adjacent spiny branchlets in cerebellar Purkinje cells lacking glutamate receptor delta 2. *J. Neurosci.* 22, 8487-8503.

Ichikawa R, Hashimoto K, Miyazaki T, Uchigashima M, Yamasaki M, Aiba A, Kano M, Watanabe M. (2016). Territories of heterologous inputs onto Purkinje cell dendrites are segregated by mGluR1-dependent parallel fiber synapse elimination. *Proc. Natl. Acad. Sci.* 113, 2282-2287.

Ito M. (1984). The cerebellum and neural control. Raven Press, New York.

Ito M, Yamaguchi K, Nagao S, Yamazaki T. (2014). Long-term depression as a model of cerebellar plasticity. *Prog. Brain Res.* 210, 1-30.

Johnson BP, Rinehart N, White O, Millist L, Fielding J. (2013). Saccade adaptation in autism and Asperger's disorder. *Neuroscience*. 243, 76-87.

Jörntell H, Hansel C. (2006). Synaptic memories upside down: bidirectional plasticity at cerebellar parallel fiber-Purkinje cell syanpses. *Neuron*. 52, 227-238.

Kaidanovich-Beilin O, Lipina T, Vukobradovic I, Roder J, Woodgett JR. (2011). Assessment of social interaction behaviors. *J. Vis. Exp.* 48, e2473.

Kakegawa W, Mitakidis N, Miura E, Abe M, Matsuda K, Takeo YH, Kohda K, Motohashi J, Takahashi A, Nagao S, Muramatsu S, Watanabe M, Sakimura K, Aricescu AR, Yuzaki M. (2015). Anterograde C1qL1 signaling is required in order to determine and maintain a single-winner climbing fiber in the mouse cerebellum. *Neuron.* 85, 316-329.

Kalueff AV, Stewart AM, Song C, Berridge KC, Graybiel AM, Fentress JC. (2015). Neurobiology of rodent self-grooming and its value for translational neuroscience. *Nature*

Reviews Neuroscience. 17, 45-59.

Kaneko M, Yamaguchi K, Eiraku M, Sato M, Takata N, Kiyohara Y, Mishina M, Hirase H, Hashikawa T, Kengaku M. (2011). Remodeling of monoplanar Purkinje cell dendrites during cerebellar circuit formation. *PLoS ONE. 6, e20108.*

Kano M, Hashimoto K, Watanabe M, Kurihara H, Offermanns S, Jiang H, Wu Y, Jun K, Shin HS, Inoue Y, Simon MI, Wu D. (1998). Phospholipase cbeta4 is specifically involved in climbing fiber synapse elimination in the developing cerebellum. *Proc. Natl. Acad. Sci.* 95, 15724-15729.

Kaufmann WE, Cooper KL, Mostofsky SH, Capone GT, Kates WR, Newschaffer CJ, Burkelis I, Stump MH, Jann AE, Landham DC. (2003). Specificity of cerebellar vermian abnormalities in autism: a quantitative magnetic resonance imaging study. *J. Child Neurol.* 18, 463-470.

Kloth AD, Badura A, Li A, Cherskov A, Connolly SG, Giovannucci A, Bangash MA, Grasselli G, Peñagarikano O, Piochon C, Tsai PT, Geschwind DH, Hansel C, Sahin M, Takumi T, Worley PF, Wang SS-H. (2015). Cerebellar associative sensory learning defects in five mouse autism models. *eLife*. 4, e06085.

Konnerth A, Dreessen J, Augustine GJ. (1992). Brief dendritic calcium signals initiate long-lasting synaptic depression in cerebellar Purkinje cells. *Proc. Natl. Acad. Sci. USA*. 89, 7051-7055.

Kühnle S, Mothes B. Matentzoglu K, Scheffner M. (2013). Role of the ubiquitin ligase E6AP/UBE3A in controlling levels of the synaptic protein arc. *Proc. Natl. Acad. Sci.* 110, 8888-8893.

Kurihara H, Hashimoto K, Kano M, Takayama C, Sakimura K, Mishina M, Inoue Y, Watanabe M. (1997). Impaired PF→PC synapse stabilization during cerebellar development of mutant mice lacking the glutamate receptor δ2 subunit. *J. Neurosci.* 17, 9613-9623.

Marr D. (1969). Theory of cerebellar cortex. *J. Physiol*. 202, 437-455.

McCormick DA, Thompson RF. (1984). Cerebellum: essential involvement in the classically conditioned eyelid response. *Science*. 223, 296-299.

Mikuni T, Uesaka N, Okuno H, Hirai H, Deisseroth K, Bito H, Kano M. (2013). Arc/Arg3.1 is a postsynaptic mediator of activity-dependent synapse elimination in the developing cerebellum. *Neuron*. 78, 1024-1035.

Miyazaki T, Hashimoto K, Shin HS, Kano M, Watanabe M. (2004). P/Q-type Ca^{2+} channel α1A regulates synaptic competition on developing cerebellar Purkinje cells. *J. Neurosci*. 24, 1734-1743.

Miyazaki T, Yamasaki M, Hashimoto K, Yamazaki M, Abe M, Usui H, Kano M, Sakimura K,

Watanabe M. (2012). Cav2.1 in cerebellar Purkinje cells regulates competitive excitatory synaptic wiring, cell survival, and cerebellar biochemical compartmentalization. *J. Neurosci.* 32, 1311-1328.

Miyazaki T, Yamasaki M, Takeuchi T, Sakimura K, Mishina M, Watanabe M. (2010). Ablation of glutamate receptor GluRdelta2 in adult Purkinje cells causes multiple innervation of climbing fibres by inducing aberrant invasion to parallel fibre innervation territory. *J. Neurosci*. 30, 15196-15209.

Moerke NJ, Aktas H, Chen H, Cantel S, Reibarkh MY, Fahmy A, Gross JD, Degterev A, Yuan J, Chorev M, Halperin JA, Wagner G. (2007). Small-molecule inhibition of the interaction between the translation initiation factors eIF4E and eIF4G. *Cell*. 128, 257-267.

Mosconi MW, Luna B, Kay-Stacey M, Nowinski CV, Rubin LH, Scudder C, Minshew N, Sweeney JA. (2013). Saccade adaptation abnormalities implicate dysfunction of cerebellar-dependent learning mechanisms in autism spectrum disorders (ASD). *PLoS ONE*. 8, e63709.

Moy SS, Nadler JJ, Perez A, Barbaro RP, Johns JM, Magnuson TR, Piven J, Crawley JN. (2004). Sociability and preference for social novelty in five inbred strains: an approach to assess autistic-like behavior in mice. *Genes, brain, and behavior*. 3, 287-302.

Najafi F, Medina JF. (2013). Beyond "all-or-nothing" climbing fibers: graded representation of teaching signals in Purkinje cells. *Front. Neural Circuits.* 7, 115.

Nakatani J, Tamada K, Hatanaka F, Ise S, Ohta H, Inoue K, Tomonaga S, Watanabe Y, Chung YJ, Banerjee R, Iwamoto K, Kato T, Okazawa M, Yamauchi K, Tanda K, Takao K, Miyakawa T, Bradley A, Takumi T. (2009). Abnormal behavior in a chromosome-engineered mouse model for human 15q11-13 duplication seen in autism. *Cell*. 137, 1235-1246.

Napoli I, Bovl PP, Eleuteri B, Zalfa F, De Rubeis S, Di Marino D, Mohr E, Massimi M, Falconi M, Witke W, Costa-Mattiolo M, Sonenberg N, Achsel T, Bagni C. (2008). The fragile X syndrome protein represses activity-dependent translation through CYFIP1, a new 4E-BP. *Cell*. 134, 1042-1054.

Nishiyama H. (2015). Dendritic translocation of climbing fibers: a new face of old phenomenon. *Cerebellum*. 14, 1-3.

Noirot E. (1966). Ultra-sounds in young rodents. I. Changes with age in albino mice. *Anim. Behav.* 14, 459-462.

Oguro-Ando A, Rosensweig C, Herman E, Nishimura Y, Werling D, Bill BR, Gao F, Coppola G, Abrahams BS, Geschwind DH. (2015). Increased CYFIP1 dosage alters cellular and dendritic morphology and dysregulates mTOR. *Mol. Psych.* 20, 1069-1078.

Okuno H, Akashi K, Ishii Y, Yagishita-Kyo N, Suzuki K, Nonaka M, Kawashima T, Fujii H,

Takemoto-Kimura S, Abe M, Natsume R, Chowdhury S, Sakimura K, Worley PF, Bito H. (2012). Inverse synaptic tagging of inactive synapses via dynamic interaction of Arc/Arg3.1 with CamKIIβ. *Cell*. 149, 886-898.

Oristaglio J, Hyman West S, Ghaffari M, Lech MS, Verma BR, Harvey JA, Welsh JP, Malone RP. (2013). Children with autism spectrum disorders show abnormal conditioned response timing on delay, but not trace, eyeblink conditioning. *Neuroscience*. 248, 708-718.

Palay SL, Chan-Palay V. (1974). *Cerebellar cortex: cytology and organization.* Springer: Berlin, Heidelberg, New York.

Palmen SJ, van Engeland H, Hof PR, Schmitz C. (2004). Neuropathological findings in autism. *Brain*. 127, 2572-2583.

Pathania M, Davenport EC, Muir J, Sheehan DF, López-Domenech G, Kittler JT. (2014). The autism and schizophrenia associated gene CYFIP1 is critical for the maintenance of dendritic complexity and the stabilization of mature spines. *Transl. Psych.* 4, e374.

Peters SU, Beaudet AL, Madduri N, Bacino CA. (2004). Autism in Angelman syndrome: implications for autism research. *Clin. Genet.* 66, 536-536.

Piochon C, Kano M, Hansel C. (2016). LTD-like molecular pathways in developmental synaptic pruning. Review. *Nat. Neurosci.* 19, 1299-1310.

Piochon C, Kloth AD, Grasselli G, Titley HK, Nakayama H, Hashimoto K, Wan V, Simmons DH, Eissa T, Nakatani J, Cherskov A, Miyazaki T, Watanabe M, Takumi T, Kano M, Wang SS, Hansel C. (2014). Cerebellar plasticity and motor learning deficits in a copy-number variation mouse model of autism. *Nat. Commun.* 5, 5586.

Piochon C, Levenes C, Ohtsuki G, Hansel C. (2010). Purkinje cell NMDA receptors assume a key role in synaptic gain control in the mature cerebellum. *J. Neurosci*. 30, 15330-15335.

Piochon C, Titley HK, Simmons DH, Grasselli G, Elgersma Y, Hansel C. (2016). Calcium threshold shift enables frequency-independent control of plasticity by and instructive signal. *Proc. Natl. Acad. Sci.* 113, 13221-13226.

Plath N, Ohana O, Dammermann B, Errington ML, Schmitz D, Gross C, Mao X, Engelsberg A, Mahlke C, Welzl H, Kobalz U, Stawrakakis A, Fernandez E, Waltereit R, Bick-Sander A, Therstappen E, Cooke SF, Blanquet V, Wurst W, Salmen B, Bösl MR, Lipp HP, Grant SG, Bliss TV, Wolfer DP, Kuhl D. (2006). Arg/Arg3.1 is essential for the consolidation of synaptic plasticity and memories. *Neuron*. 52, 437-444.

Purves D, Augustine GJ, Fitzpatrick D, et al. (2001). Neuroscience. 2nd edition. Sunderland (MA): Sinauer Associates. Projections to the Cerebellum.

Reeb-Sutherland BC, Fox NA. (2015). Eyeblink conditioning: a non-invasive biomarker for

neurodevelopmental disorders. *J. Autism Dev. Disord.* 45, 376-394.

Reissner C, Runkel F, Missler M. (2013). Neurexins. *Genome Biol.* 14, 213-228.

Rogers SJ, Wehner DE, Hagerman R. (2001). The behavioral phenotype in fragile X: symptoms of autism in very young children with fragile X syndrome, idiopathic autism, and other developmental disorders. *J. Dev. Behav. Pediatr.* 22, 409-417.

Rossi F, Borsello T, Vaudano E, Strata P. (1993). Regressive modifications of climbing fibres following Purkinje cell degeneration in the cerebellar cortex of the adult rat. *Neuroscience*. 53, 759-778.

Sakuri M. (1987). Synaptic modification of parallel fiber-Purkinje cell transmission in *in vitro* guinea-pig cerebellar slices. *J. Physiol.* 394, 463-480.

Sakuri M. (1990). Calcium is an intracellular mediator of the climbing fiber in induction of cerebellar long-term depression. *Proc. Nat. Acad. Sci.* 87, 3383-3385.

Sandin S, Lichtenstein P, Kuja-Halkola R, Hultman C, Larsson H, Reichenberg A. (2017). The heritability of autism spectrum disorder. *JAMA*. 318, 1182-1184.

Santini E, Huynh TN, MacAskill AF, Carter AG, Pierre P, Ruggero D, Kaphzan H, Klann E. (2013). Exaggerated translation causes synaptic and behavioral aberrations associated with autism. *Nature*. 493, 411-415.

Scattoni ML, Crawley J, Ricceri L. (2009). Ultrasonic vocalizations: A tool for behavioural phenotyping of mouse models of neurodevelopmental disorders. *Neurosci. Biobehav. Rev.* 33, 508-515.

Schenck A, Bardoni B, Moro A, Bagni C, Mandel JL. (2001). A highly conserved protein family interacting with the fragile X mental retardation protein (FMRP) and displaying selective interactions with FMRP-related proteins FXR1P and FXR2P. *Proc. Natl. Acad. Sci. USA*. 98, 8844-8849.

Schonewille M, Belmeguenai A, Koekkoek SK, Houtman SH, Boele HJ, van Beugen BJ, Gao Z, Badura A, Ohtsuki G, Amerika WE, Hosy E, Hoebeek FE, Elgersma Y, Hansel C, De Zeeuw CI. (2010). Purkinje cell-specific knockout of the protein phosphatase PP2B impairs potentiation and cerebellar motor learning. *Neuron*. 67, 618-628.

Sears LL, Finn PR, Steinmetz JE. (1994). Abnormal classical eye-blink conditioning in autism. *J. Autism Dev. Disord*. 24, 737-751.

Shibuki K, Okada D. (1992). Cerebellar long-term potentiation under suppressed postsynaptic Ca^{2+} activity. *Neuroreport*. 3, 231-234.

Silverman JL, Yang M, Lord C, Crawley JN. (2010). Behavioural phenotyping assays for mouse

models of autism. *Nat. Rev. Neuro.* 11, 490-502.

Simmons DH, Titley HK, Hansel C, Mason P. (2018). Behavioral tests for mouse models of Autism Spectrum Disorder: a critical evaluation. *[in preparation]*.

Simmons DH, Titley HK, Piochon C, Longo F, Vorobyeva A, Grasselli G, Santini E, Takumi T, Geschwind D, Klann E, Hansel C. (2018). Deficient calcium signaling in aberrant glutamatergic cerebellar synaptic physiology in the 15q11-13 and CYFIP1 OE murine models of ASD. *[in preparation]*.

Simpson JI, Wylie DR, De Zeeuw CI. (1996). On climbing fiber signals and their consequence(s). *Behav. Brain Sci.* 19, 384-398.

Smith SEP, Zhou YD, Zhang G, Jin Z, Stoppel DC, Anderson MP. (2011). Increased gene dosage of *Ube3a* results in autism traits and decreased glutamate synaptic transmission in mice. *Sci. Transl. Med*. 3, 103.

Steinlin M & Wingeier K. (2013). Cerebellum and cognition. (Dordrecht: Springer).

Strick PL, Dum RP, Flez JA. (2009). Cerebellum and nonmotor function. *Annu. Rev. Neurosci.* 32, 413-434.

Sugihara I, Wu H, Shinoda Y. (1999). Morphology of single olivocerebellar axons labeled with biotinylated dextran amine in the rat. *J. Comp. Neurol.* 414, 131-148.

Tang G, Gudsnuk K, Kuo S, Cotrina ML, Rosoklija G, Sosunov A, Sonders MS, Kanter E, Castagna C, Yamamoto A, Yue Z, Arancio O, Peterson BS, Champagne F, Dwork AJ, Goldman J, Sulzer D. (2014). Loss of mTOR-dependent macroautophagy causes autistic-like synaptic pruning deficits. *Neuron*. 83, 1131-1143.

Uesaka N, Abe M, Konno K, Yamazaki M, Sakoori K, Watanabe T, Kao T, Mikuni T, Watanabe M, Sakimura K, Kano M. (2018). Retrograde signaling from progranulin to sort1 counteracts synapse elimination in the developing cerebellum. *Neuron.* 97, 796-805.

Uesaka N, Uchigashima M, Mikuni T, Nakazawa T, Nakao H, Hirai H, Aiba A, Watanabe M, Kano M. (2014). Retrograde semaphoring signaling regulates synapse elimination in the developing mouse brain. *Science Express*. 344, 1020-1023.

Urraca N, Cleary J, Brewer V, Pivnick EK, McVicar K, Thibert RL, Schanen NC, Esmer C, Lamport D, Reiter LT. (2013). The interstitial duplication 15q11.2-q13 syndrome includes autism, mild facial anomalies and a characteristic EEG signature. *Autism Res.* 6, 268-279.

Uzunova G, Pallanti S, Hollander E. (2016). Excitatory/inhibitory imbalance in autism spectrum disorders: Implications for interventions and therapeutics. *World J. Biol. Psychiatry.* 17, 174-186.

van Beugen BJ, Qiao X, Simmons DH, De Zeeuw CI, Hansel C. (2014). Enhanced AMPA

receptor function promotes cerebellar long-term depression rather than potentiation. *Learn. Mem.* 21, 1-7.

Waltes R, Gfesser J, Haslinger D, Schneider-Momm K, Biscaldi M, Voran A, Freitag CM, Chiocchetti AG. (2014). Common eIF4E variants modulate risk for autism spectrum disorders in the high-functioning range. *J. Neural. Transm.* 121, 1107-1116.

Wang H, Ardiles AO, Yang S, Tran T, Posada-Duque R, Valdivia G, Baek M, Chuang Y, Palacios AG, Gallagher M, Worley P, Kirkwood A. (2016). Metabotropic glutamate receptors induce a form of LTP controlled by translation and Arc signaling in the hippocampus. *J. Neurosci*. 36, 1723-1729.

Wang SS-H, Kloth AD, Badura A. (2014). The cerebellum, sensitive periods, and autism. *Neuron*. 83, 518-532.

Watanabe M. (2008). Molecular mechanisms governing competitive synaptic wiring in cerebellar Purkinje cells. *Tohoku J. Exp. Med.* 214, 175-190.

Wegiel J, Kuchna I, Nowicki K, Imaki H, Wegiel J, Ma SY, Azmitia EC, Banerjee P, Flory M, Cohen IL, London E, Brown WT, Komich Hare C, Wisniewski T. (2013). Contribution of olivofloccular circuitry developmental defects to atypical gaze in autism. *Brain Res.* 1512, 106-122.

Zoghbi HY, Bear MF. (2012). Synaptic dysfunction in neurodevelopmental disorders associated with autism and intellectual disabilities. *Cold Spring Harb. Perspect. Biol.* 4, a009886.